A global algorithm for identifying changing streamflow regimes: Application to Canadian natural streams (1966-2010)

Masoud Zaerpour[1], Shadi Hatami[1], Javad Sadri[2] and Ali Nazemi[1]

[1]Department of Building, Civil and Environmental Engineering, Concordia University, Montreal, Quebec, Canada

[2]Oppimi Group, Montréal, Quebec, Canada

Correspondence to: Masoud Zaerpour (masoud.zaerpour@concordia.ca)

Abstract. Climate change affects natural streamflow regimes globally. To assess temporal alterations in the streamflow regime, typically variations in one or few streamflow characteristics are taken as a notion of regime change. This approach, however, cannot see simultaneous changes in multiple streamflow characteristics, does not utilize all the available information contained in a streamflow hydrograph, and cannot describe how and to what extent streamflow regimes evolves to one another. To address these gaps, we conceptualize streamflow regimes as intersecting spectrums that are formed by multiple streamflow characteristics. Accordingly, we recognize that changes in a streamflow regime should be diagnosed through gradual, yet continuous changes in an ensemble of streamflow characteristics. To incorporate these key considerations, we propose a generic algorithm to first classify streams into a finite set of intersecting fuzzy clusters. Accordingly, by analyzing how the degrees of membership to each cluster change, we quantify temporal shifts from one regime to another in a given stream. Our proposed algorithm eliminates the subjectivity in identifying regime types and quantifying shifts between streamflow regimes. We apply this approach to the data, obtained from 105 natural Canadian streams, during the period of 1966 to 2010. We show that natural streamflow in Canada can be categorized into six regime types, with clear physical and geographical distinctions. Analyses of trends in membership values show that alterations in natural streamflow regime vary among different regions. Having said that, we show that in more than 80% of considered streams, there is a dominant regime shift that can be attributed to simultaneous changes in streamflow characteristics, some of which have remained previously unknown. Our study not only introduces a new algorithmic framework for identifying changing streamflow regimes at regional and global scales, but also provides a fresh look at streamflow alterations in Canada and reveals the complex and multifaceted impacts of climate change on streamflow regimes in cold regions.

1 Introduction

Natural characteristics of streamflow are critical to ecosystem livelihood and human developments around river systems (Poff et al., 2010; Nazemi and Wheater, 2014; Hassanzadeh et al., 2017). Since early settlements, humans have considered seasonality, variability, and magnitude of natural streamflow as key factors for determining socio-economic developments (Knouft and Ficklin, 2017). While some streamflow characteristics reveal potentials for agriculture and energy production

(Hamududu and Killingtveit, 2012; Amir Jabbari and Nazemi, 2019; Nazemi et al., 2020), some determine the consequences of devastating disasters such as floods or droughts (Arheimer and Lindström, 2015; Burn and Whitfield, 2016; Zandmoghaddam et al., 2019).

A set of streamflow characteristics, collectively defining the overall flow behavior in a river reach, is called the streamflow regime (Poff et al., 1997). Traditionally, streamflow regimes have been considered stationary in time (Milly et al. 2008). However, the looming effects of climate change along with human interventions in river systems through land and water management have raised fundamental questions regarding the feasibility of stationarity assumption during the current "*Anthropocene*" (Arnell and Gosling, 2013; Nazemi and Wheater, 2015a, 2015b). Even in undisturbed streams, recent literature is full of evidence, revealing major alterations induced by heightened climate variability and change (Barnett et al., 2005; Stahl et al., 2010; Rood et al., 2016; Hodgkins et al., 2017; Dierauer et al., 2018), with increasing rates in years to come (Asadieh, and Krakauer, 2017). Assessing how streamflow regime is changing as a result of alterations in natural and anthropogenic drivers is currently one of the imminent questions in the field of hydrology.

Despite the extensive body of knowledge already gathered around assessing the effects of climate change on altering streamflow regimes, there are still rooms for methodological developments. Most importantly, among many potential flow characteristics that can constitute and describe streamflow regime, often only a few are taken into account (Whitfield and Cannon, 2000; Hall et al., 2014; Vormoor et al., 2015). This is a technical limitation because climate change impacts are often manifested in the entire streamflow hydrograph, and not only around certain streamflow characteristics (Olden and Poff, 2003). This is due to the fact that at the watershed scale, multiple processes contribute to the streamflow generation, each behaving differently in response to climate variability and change (Whitfield and Pomeroy, 2016). This is particularly the case in cold regions, where recent alterations in streamflow regimes are not only significant (e.g., Déry and Wood, 2005; MacDonald et al., 2018; Islam et al., 2019; Champagne et al., 2020); but also it is complex, due to compound impacts of changes in temperature, shifts in forms and magnitude of precipitation, as well as alterations in snow/ice accumulation and melt (DeBeer et al., 2016; Hatami et al., 2018; Rottler et al., 2020). At this stage of development, it is not possible to systematically quantify streamflow regimes and their alterations to one another using a large set of simultaneously changing streamflow characteristics (Burn et al., 2016; Burn and Whitfield, 2018).

Here, we propose a new methodology to address this challenge. We recognize that by considering more streamflow characteristics, the distinctions between regime types and their alterations become more fuzzy and relative. Accordingly, in line with some recent suggestions in the literature (see e.g., Ternynck et al., 2016; Burn and Whitfield, 2017; Knoben et al., 2018; Brunner et al., 2018, 2019; Aksamit and Whitfield, 2019; Jehn et al., 2020), we conceptualize streamflow regimes as continuous spectrums rather than distinct states. This conceptualization requires a methodology that can formally deal with relativity in the definition of a streamflow regime and its alterations in time and space. For this purpose, we use elements of fuzzy set theory (see Zadeh, 1965; Nazemi et al., 2002) to provide a methodological basis to classify streamflow regimes as intersecting clusters. We then measure the gradual departure from one fuzzy cluster to others using significant monotonic trends in membership degrees and use this information as an indicator for a regime shift in a given stream. Accordingly, we highlight how such regime shifts are attributed to changes in streamflow characteristics using a formal dependence analysis.

We implement this algorithm in Canada, where the rate of warming is twice the global average (Bush and Lemmen, 2019), and changes in streamflow characteristics are significant in time and space (e.g., Buttle et al., 2016; O'Neil et al., 2017; Dierauer et al., 2020). By considering more than 100 natural streams from coast to coast to coast during a unified period, we provide a homogeneous, pan-Canadian view on recent alterations in natural streamflow regimes across the country. The remainder of this paper is as the following: Section 2 describes our three-step methodology related to (i) clustering regime types, (ii) detecting regime changes, and (iii) attributing regime changes to alterations in streamflow characteristics. Section 3 introduces our case study and the data. The results and discussions are presented in Sects 4 and 5, respectively. Finally, Sect. 6 concludes our work and provides some further remarks.

2 Methodology

2.1 Rationale and proposed algorithm

From both conceptual and computational perspectives, quantifying changes in streamflow regimes is not a trivial task due to multifaceted definitions of streamflow regimes, which are subject to relativity. On the one hand, the flow regime at a given stream is defined by a large number of streamflow characteristics, some of which with conflicting dynamics in time and space. On the other hand, the flow regime is often identified based on similarity/dissimilarity with characteristics in a set of benchmarking streams with known regimes. Accordingly, regime shifts are not only defined based on alterations in streamflow characteristics relative to the past, but also with respect to relative changes with respect to other streams with known regime types. This makes a complex mathematical problem due to the "*curse of dimensionality*" (see e.g., Trunk 1979), meaning that the complexity of the problem increases exponentially by increasing the number of streams and/or streamflow characteristics, with which the streamflow regime is defined. To solve this problem, the general tendency in the literature is to reduce the dimensionality of the problem through the use of methodologies, such as Multi-Dimensional Scaling (MDS), Empirical Orthogonal Functions (EOFs), and Principal Component Analysis (PCA) to name a few (Maurer et al., 2004; Johnston and Shmagin, 2008). Despite methodological differences, all these approaches try to provide a parsimonious representation of a hyperdimensional space by creating a much simpler space that can preserve the variability of the original hyperspace in its domain (Guetter and Georgakakos, 1993). Although these methodologies are able to substantially reduce the dimensionality and give valuable insights into changes in hyper dimensional data sets, the results are hard to interpret, particularly when attribution to some physical characteristics are concerned (Matalas and Reiher, 1967; Overland and Preisendorfer, 1982; Hannachi et al., 2009 and references therein). In the case of quantifying changes in streamflow regimes, this limitation translates into an inability to attribute the formation and transition in regime types directly to a set of specific streamflow characteristics.

Here, we aim at addressing this problem through a new methodology that does not rely on dimension reduction; rather, it tries to embrace the inherent hyper-dimensionality of the problem. Below we suggest an integrated approach , (1) to classify natural streamflow regimes into a set of interpolating regime types, (2) to diagnose the gradual evolution in regime types and their shifts in time, and (3) to attribute changes in streamflow regimes to alterations in streamflow characteristics. Figure 1 shows the proposed three-step procedure. We use MATLAB® Programming platform for the implementation of this algorithmic procedure.

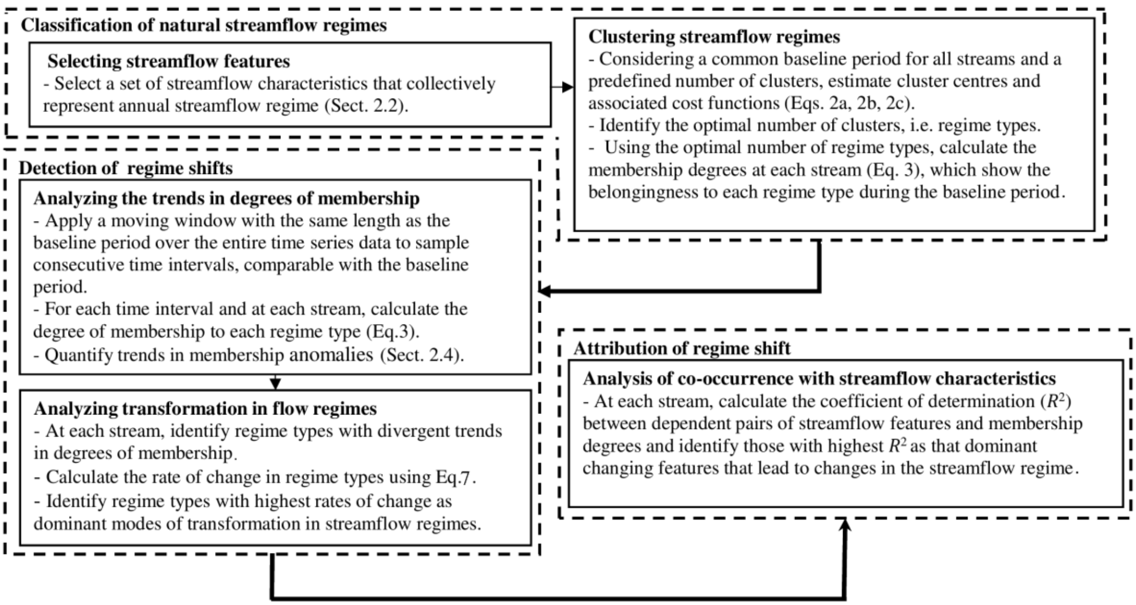

Figure 1. The workflow of the proposed algorithm for classifying streamflow regime, diagnosing shift in streamflow regime, and attributing the regime shift to the changes in streamflow characteristics.

Our approach is built upon two fundamental considerations. First, we acknowledge that streamflow regimes are constituted by several streamflow characteristics, and therefore changes in streamflow regimes are manifested through changes in an ensemble of streamflow characteristics. Second, we recognize that there are soft as oppose to hard distinctions between streamflow regimes; and, regime shifts occur gradually rather than abruptly. These two considerations lead to the development of our proposed algorithm. In brief, we select a set of streamflow characteristics – or features – to collectively characterize the streamflow regime. We then use the Fuzzy C-Means algorithm (FCM) to classify streams into a set of overlapping regime types during a common baseline period. We accordingly quantify changes in degrees of association to each regime type during the entire data period using a moving trend analysis. By monitoring the co-occurrence of divergent trends in membership values, the transitions of regime types to one another can be identified. Finally, we monitor the co-evolution of regime shifts with the alterations in streamflow characteristics through a formal dependency analysis.

2.2 Feature selection

Indicators of Hydrologic Alterations (IHAs: Richter et al., 1996) are commonly applied as *features* to characterize changes in natural streamflow regimes (e.g., Wang et al., 2018). Different sets of IHAs can be considered to constitute streamflow regimes depending on the application at hand. Here we consider 15 IHAs, including annual mean flow, monthly mean flows as well as timings of the annual low and high flows that together can represent the shape of the annual hydrograph. At each stream, we use the mean (first moment) and variance (second moment) of these 15 indicators during a multi-year timeframe to come up with 30 features that together can capture the shape of the long-term annual hydrograph and the inter-annual variability around it. Table 1 shows the name and notation of the features used, where $x_{j=1:15}$ and $y_{j=1:15}$ denote the mean and the variance of the 15 IHAs, respectively.

Table 1. The thirty streamflow features used for clustering natural streamflow regime in Canada.

Feature	Notation	Feature	Notation	Feature	Notation	Feature	Notation	Feature	Notation
October mean flow	mean: x_1 variance: y_1	November mean flow	mean: x_2 variance: y_2	December mean flow	mean: x_3 variance: y_3	January mean flow	mean: x_4 variance: y_4	February mean flow	mean: x_5 variance: y_5
March mean flow	mean: x_6 variance: y_6	April mean flow	mean: x_7 variance: y_7	May mean flow	mean: x_8 variance: y_8	June mean flow	mean: x_9 variance: y_9	July mean flow	mean: x_{10} variance: y_{10}
August mean flow	mean: x_{11} variance: y_{11}	September mean flow	mean: x_{12} variance: y_{12}	Annual flow	mean: x_{13} variance: y_{13}	Timing of the annual low flow	mean: x_{14} variance: y_{14}	Timing of the annual high flow	mean: x_{15} variance: y_{15}

2.3 Fuzzy C-means clustering

Clustering is the process of arranging data into a finite set of classes, in a way that members in the same class have similar characteristics. Statistical methodologies used for clustering in hydrology are numerous (see Tarasova et al., 2019; Brunner et al., 2020) and have been traditionally limited to non-overlapping (i.e. hard) classes (Olden et al., 2012). Recent theoretical developments have relaxed this assumption and considered a set of overlapping (i.e. soft) classes, in particular in the form of fuzzy clusters (e.g., Knoben et al., 2018; Wolfe et al., 2019). The association to each fuzzy cluster can be quantified using a degree of belongingness, also known as the membership value (see Bezdek, 1981; Sikorska et al., 2015). The process of clustering streamflow regime using FCM can be summarized as the following: Assume that streamflow data from N hydrometric gauges during a common timeframe w with the length of l years are available. For each stream, the first and second moments of n IHAs (here $n = 15$), i.e. $\mathbf{X} = [x_{ij}],\ \mathbf{Y} = [y_{ij}];\ i \in \{1, \ldots, N\},\ j \in \{1, \ldots, n\}$, can be extracted during the timeframe w. The extracted features should be normalized to avoid scale mismatches in the feature matrix:

$$\bar{x}_{i,j} = \frac{x_{i,j} - \mathbf{min}\{x_{i=1:N,j}\}}{\mathbf{max}\{x_{i=1:N,j}\} - \mathbf{min}\{x_{i=1:N,j}\}} \quad \forall\, j \in \{1, \ldots, n\} \tag{1a}$$

$$\bar{y}_{i,j} = \frac{y_{i,j} - \mathbf{min}\{y_{i=1:N,j}\}}{\mathbf{max}\{y_{i=1:N,j}\} - \mathbf{min}\{y_{i=1:N,j}\}} \quad \forall\, j \in \{1, \ldots, n\} \tag{1b}$$

where $\bar{\mathbf{X}} = [\bar{x}_{ij}]$ and $\bar{\mathbf{Y}} = [\bar{y}_{ij}]$ are the matrices of Normalized Streamflow Features (NSFs). FCM partitions the N streams into c fuzzy clusters, such that the sum of distances for all streams $i \in \{1, \ldots, N\}$ between NSFs and cluster centroids is minimized. This is often formulated through an iterative optimization procedure, aiming at finding the cluster centroid by minimizing the following objective function:

$$\boldsymbol{J}(\mathbf{U}, \mathbf{V}\,|\bar{\mathbf{X}}, \bar{\mathbf{Y}}) = \sum_{k=1}^{c} \sum_{i=1}^{N} (u_{i,k})^2 \boldsymbol{d}^2([\bar{x}_{i,j=1:n}\bar{y}_{i,j=1:n}]\,, v_{k,m=1:2n}) \tag{2a}$$

This objective function is subject to the following two constraints:

$$\sum_{k=1}^{c} u_{i,k} = 1 \quad \forall\, i \in \{1, \ldots, N\} \tag{2b}$$

$$0 < \sum_{i=1}^{N} u_{i,k} < N \quad \forall\, k \in \{1, \ldots, c\} \tag{2c}$$

where $\mathbf{V} = v_{k=1:c,m=1:2n} = \left[\overline{x^*}_{k,j=1:n}, \overline{y^*}_{k,j=1:n}\right] = [\overline{x^*}_{k,1}, \ldots, \overline{x^*}_{k,n}, \overline{y^*}_{k,1}, \ldots, \overline{y^*}_{k,n}] \in \mathbb{R}^{2n}$ is the matrix of cluster centroids (i.e., regime types); the matrix of $\mathbf{U} = [u_{i,k}]; i \in \{1, \ldots, N\}, k \in \{1, \ldots, c\}$ is the matrix of memberships; and $\boldsymbol{d}^2([\bar{x}_{i,j=1:n}, \bar{y}_{i,j=1:n}], v_{k,m=1:2n})$ is the matrix of squared Euclidian distances between NSFs of stream i and clusters' centroid k. The fuzzy membership matrix can be accordingly calculated as:

$$u_{ik} = \frac{\left(\frac{1}{\boldsymbol{d}^2([\bar{x}_{i,j=1:n}\bar{y}_{i,j=1:n}], v_{k,m=1:2n})}\right)}{\sum_{k=1}^{c}\left(\frac{1}{\boldsymbol{d}^2([\bar{x}_{i,j=1:n}\bar{y}_{i,j=1:n}], v_{k,m=1:2n})}\right)};\ \ i \in \{1, \ldots, N\}, k \in \{1, \ldots, c\} \tag{3}$$

The number of clusters c (here regime types) can be chosen as a *priori*, or empirically using validity indices (Srinivas et al., 2008). Here, we implement three validity indices of Xie-Beni index (V_{XB}; Xie and Beni, 1991), partition index (V_{SC}; Bensaid et al., 1996), and separation index (V_S; Fukuyama and Sugeno, 1989) to come up with an optimal number of clusters. These indices are based on two criteria, namely compactness and separation. The compactness characterizes how close members to each cluster are; whereas, the separation measures how distinct two clusters are. A good clustering result should have both small intra-cluster compactness and large inter-cluster separation.

The Xie-Beni validity index is the ratio of compactness to the separation, quantified by the average of fuzzy variation of NSFs from clusters' centroids to the minimum squared distance between cluster centroids:

$$V_{XB} = \frac{\sum_{k=1}^{c}\sum_{i=1}^{N}\left(u_{i,k}\right)^2 \boldsymbol{d}^2\left(\left[\bar{x}_{i,j=1:n}, \bar{y}_{i,j=1:n}\right], v_{k,m=1:2n}\right)}{N \times \min_{k,\ l \neq k}\left(\boldsymbol{d}^2\left(\left[v_{l,m=1:2n}, v_{k,m=1:2n}\right)\right)\right.} \tag{4}$$

where $\sum_{i=1}^{N}\left(u_{i,k}\right)^2 \boldsymbol{d}^2\left(\left[\bar{x}_{i,j=1:n}, \bar{y}_{i,j=1:n}\right], v_{k,m=1:2n}\right)$ is the compactness of fuzzy cluster *k* and separation of fuzzy clusters is quantified by the minimum squared Euclidean distance between cluster centroids.

Partition index is quantified by the sum of *individual* fuzzy cluster variations (i.e., the compactness of fuzzy clusters) to the sum of the distances from cluster centroids (i.e., the separation of fuzzy clusters). This ratio is further normalized by fuzzy cardinality weight γ_k, defined by $\gamma_k = \sum_{i=1}^{N} u_{i,k}$, to avoid the bias made by cluster sizes.

$$V_{SC} = \sum_{k=1}^{c}\left\{\frac{\sum_{i=1}^{N}\left(u_{i,k}\right)^2 \boldsymbol{d}^2\left(\left[\bar{x}_{i,j=1:n}, \bar{y}_{i,j=1:n}\right], v_{k,m=1:2n}\right)}{\gamma_k \times \sum_{l=1}^{c} \boldsymbol{d}^2\left(v_{l,m=1:2n}, v_{k,m=1:2n}\right)}\right\} \tag{5}$$

The separation index, also known as Fukuyama and Sugeno index, is defined based on the difference between the compactness and the separation of fuzzy clusters:

$$V_S = \left\{\sum_{k=1}^{c}\sum_{i=1}^{N} u_{i,k}^2 \cdot \boldsymbol{d}^2\left(\left[\bar{x}_{i,j=1:n}, \bar{y}_{i,j=1:n}\right], v_{k,m=1:2n}\right)\right\} - \left\{\sum_{k=1}^{c}\sum_{i=1}^{N} u_{i,k}^2 \cdot \boldsymbol{d}^2\left(\left[v_{k,m=1:2n}, \bar{v}\right)\right.\right\} \tag{6}$$

in which $\bar{v} = \sum_{k=1}^{c} v_i / c$. We identify the optimal number of clusters using the elbow method (see Satopaa et al., 2011; Kuentz et al., 2017), which involves finding the maximum number of clusters, beyond which slopes of improvement in validity indices flatten significantly; and adding a new cluster does not justify the increased complexity.

2.4 Detection of change in streamflow regimes

Clustering natural streams into c regime types takes place during a baseline timeframe with the length of l years, in which the optimal number of clusters, cluster centroids, and initial membership degrees to each regime type are identified. For each stream, the timeframe can be moved year-by-year and the membership values can be recalculated for the new window using Eq. (3). Figure 2 exemplifies this process in a hypothetical case. This results into c time series of membership degrees at each stream, showing how the association to each regime type evolves in time – see Jaramillo and Nazemi (2018) for more details on moving window methodology. In order to quantify the gradual change in membership degrees, the Mann-Kendall trend test with the Sen's Slope is applied (Mann, 1945; Sen, 1968; Kendall, 1975).

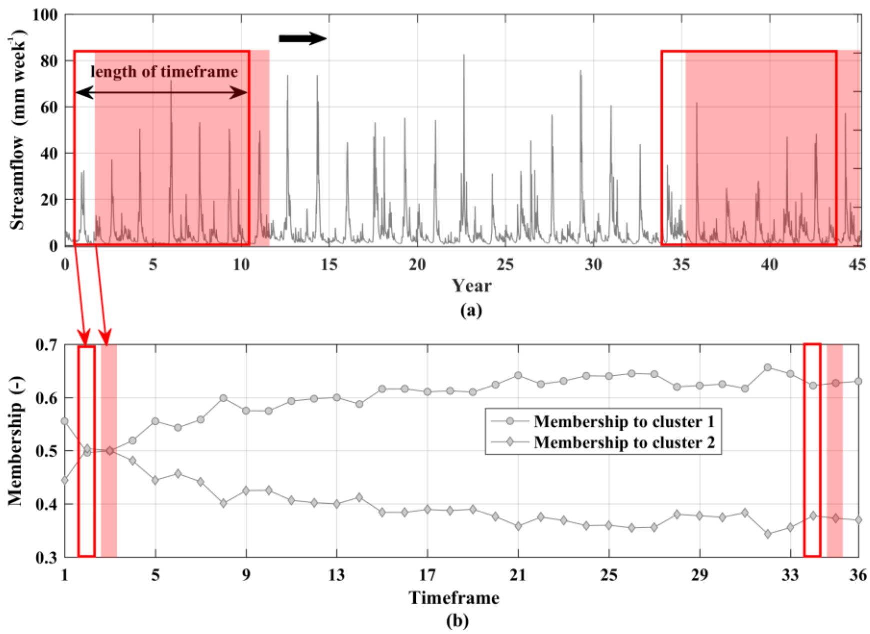

Figure 2. A schematic view to the procedure of identifying the evolution in membership values using a moving window; (a) a decadal timeframe slides over the streamflow time series year-by-year; (b) membership degrees are recalculated at each decadal timeframe to systematically determine the changes in association to each regime type determined in the beginning of the data period.

As the sum of memberships in each timeframe is one (see Eq. 2b), a gradual increase in memberships to one cluster (positive trend) should coincide with a gradual decrease in the membership of one or more clusters (negative trend). At each stream, this transition can be identified by significant negative dependencies between membership degrees of two clusters.

Assuming the pair of clusters p and q in stream i, the rate of shift from p to q can be quantified using Eq. 7, where $u_{i,p}(w)$ and $u_{i,q}(w)$ are membership degrees to clusters p and q in stream i during the timeframe w; $w \in \{1, \ldots, r\}$; r is the number of moving timeframes needed to cover the whole data period year-by-year; $\mathbf{E}(u_{i,p})$ and $\mathbf{E}(u_{i,q})$ are the expected memberships; and $S_{i,(p,q)}$ is the slope of the best-fitted line.

$$S_{i,(p,q)} = \left| \frac{\sum_{w=1}^{m} \left(u_{i,q}(w) - \mathbf{E}(u_{i,q})\right)\left(u_{i,p}(w) - \mathbf{E}(u_{i,p})\right)}{\sum_{w=1}^{m} \left(u_{i,q}(w) - \mathbf{E}(u_{i,q})\right)^2} \right| \tag{7}$$

for $1 \le w \le m$ and $1 \le p, q \le c \; and \; p \ne q \quad \forall \, i \, \in \{1, \ldots, N\}$

2.5 Attribution of change in streamflow regime to alterations in streamflow characteristics

Here, we recognize that the existence of significant dependence between membership values and streamflow features can provide a systematic way to detect attribution. Accordingly, we use Kendall's tau (Genest and Favre, 2007; Nazemi and Elshorbagy, 2012) to detect the co-occurrence between changes in memberships and changes in NSFs. Figure 3 shows the procedure of attribution. Left panels show the changes in membership degrees of two hypothetical clusters (purple lines), along with the corresponding changes in two NSFs (grey lines). Right panels show the scatter plots of membership degrees *vs.* the NSFs. We identify the significance and the direction of dependence using the Kendall's tau coefficient. Independently, to measure the linear association between changes in streamflow features $x_{i,j}$ and membership values $u_{i,k}$, the coefficient of determination (R^2; see Legates and McCabe Jr., 1999) is used. R^2 varies between [0, 1] and determines how much of the variability in the degrees of membership can be described by the variability in a given streamflow characteristics. The higher the R^2 is, the stronger the association between changes in degrees of membership and the considered streamflow characteristics is. The coefficient of determination in this case can be calculated as:

$$R^2(u_{i,k}, x_{i,j}) = \frac{\left\{\sum_{w=1}^{r} \left(u_{i,k} - \mathbf{E}(u_{i,k})\right)\left(x_{i,j} - \mathbf{E}(x_{i,j})\right)\right\}^2}{\sum_{w=1}^{r} \left(u_{i,k} - \mathbf{E}(u_{i,k})\right)^2 \sum_{w=1}^{r} \left(x_{i,j} - \mathbf{E}(x_{i,j})\right)^2} \quad \forall \, i \, \in \{1, \ldots, N\} \tag{8}$$

By the simultaneous use of Kendall's tau and R^2, we try to facilitate quantitative communication of the impact of changes in a specific streamflow characteristic on the transition from one regime type to another. On the one hand, by using the Kendall's tau, we identify the sign and significance of dependencies between changes in membership degrees and changes in streamflow characteristics using a non-parametric approach that can handle non-linearity in the form of association. Using R^2 on the other hand, we quantify how much of the variance in the membership degrees can be described by the variance in the changes in streamflow characteristics. This is to provide a comprehendible measure of association between the two quantities.

The key advantage of our proposed algorithm is in its transparency and the fact that the detection of a change in streamflow regime is tied up with attribution to changes in streamflow characteristics. Figure 4 shows this integration using a hypothetical example. The left panel demonstrates a multifaceted change in the shape of the annual hydrograph in a given stream during two separate periods, shown with grey and pink envelopes. Black and red lines are the expected annual hydrographs for each envelope, respectively. Any shift between flow regimes should be revealed by at least a pair of membership timeseries with opposite trends. The strength of the link is measured using R^2. The right panel shows the rates of shifts and the attribution to changes in streamflow characteristics using gray links. The thickness of links is proportional to rates of shift and/or R^2 values.

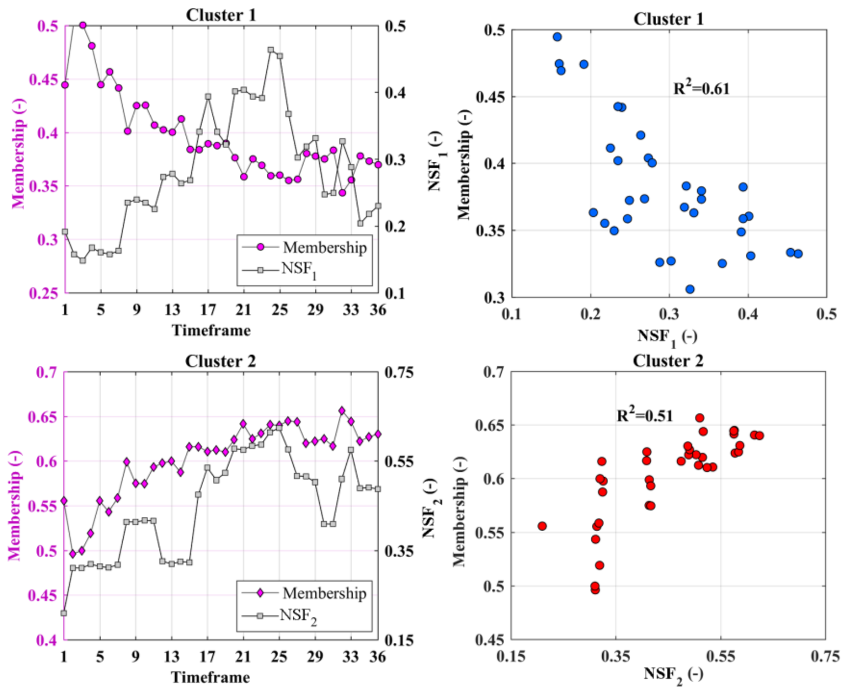

Figure 3. The procedure of attributing changes in membership degrees to changes in streamflow characteristics. The left column shows the co-evolution of membership degrees and Normalized Streamflow Features. The right column measures the correspondence between changes in membership degrees and normalized streamflow features through percentage of described variance quantified using R^2. Red or blue dots show the positive or negative dependencies, respectively.

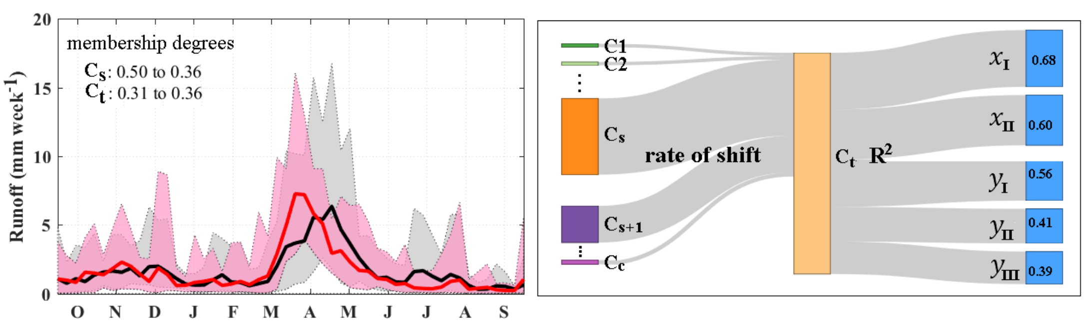

Figure 4. An example for transitions between regime types along with attribution of change to streamflow characteristics. The left panel shows annual hydrographs in two separate periods using grey and pink envelopes. The panel in the right shows the dominant shift in the flow regime by maximum rate of shift, and attributes this shift to changes in significantly dependent streamflow characteristics. The dominant shift is visualized by the thickest grey envelope. The strength of the association between regime shift and significantly dependent streamflow characteristics are measured and communicated by R^2.

3 Case study and data

With the total catchment area equivalent to 6% of the global land area, Canadian rivers roll coast to coast to coast and during their journey support important socio-economic activities such as agriculture and hydropower production. River systems in Canada can be divided into four major ocean-drained basins, namely Pacific, Atlantic, Arctic, and Hudson Bay that can be further divided into a number of sub-basins (Pearse et al., 1985; Natural Resources Canada, 2007). The Pacific basin spreads on the west coast, from the US border to Yukon, is the smallest among all, draining around 1 million km^2. The main sub-basins in the Pacific include Fraser, Yukon, Columbia, and the Seaboard. In the east coast, the Atlantic basin drains a total area of 1.6 million km^2, and includes important water bodies such as the Great Lakes. The basin includes three sub-basins, namely the St. Lawrence River, Seaboard, and the Saint John-St. Croix. Towards the north, the Arctic basin drains over 3.5 million km^2 of northern lands and includes some of Canada's largest water bodies such as the Slave, Athabasca, and Great Bear lakes. Mackenzie, Peace-Athabasca, and Seaboard are the main sub-basins in the Arctic basin. With an area of 3.8 million km^2, the Hudson Bay is the largest drainage basin in Canada, covering five provinces from Alberta in the west to Québec in the east. The basin includes four major sub-basins, namely Western & Northern Hudson Bay, Nelson, Northern Ontario, and Northern Québec. Nelson, Saskatchewan, and Churchill rivers are the major river systems in the Hudson Bay.

While drainage basins are often used as the unit in which the streamflow is traced from headwaters to oceans, there are substantial differences within a drainage basin in terms of climate, topography, vegetation, geology, and land use. This results into multiple forms of hydrological response within one drainage basin. In contrast to drainage basins, terrestrial ecozones are identified based on similarity in climate and land characteristics; and therefore, they can be more representative of different hydrological responses (Whitfield 2000). In brief, an ecozone is a patch of terrestrial land with distinc climatic, ecologic, and aquatic characteristics (see Wiken 1986; Marshall et al., 1999; Wong et al., 2017). Canada includes 15 ecozones. Starting from the north, the Arctic Cordillera (EZ1), covering 2% of Canada's landmass, contains the only major Canadian region outside the Rockies. The Northern Arctic (EZ2) is equivalent to 14% of Canada's landmass and mainly covers Arctic Islands (Coops et al., 2008). The Southern Arctic ecozone (EZ3) includes the northern mainland, covering 8% of Canada. The Taiga Plains (EZ4) with a large number of wetlands, extended mainly on the western side of the Northwest Territories, covering 6% of Canada's landmass. Taiga Shield (EZ5) with large number of lakes, covers 13% of Canada's landmass in the south of the Southern Arctic (Marshall et al., 1999). The Boreal Shield (EZ6) is Canada's largest ecozone by covering 18% of the country's landmass, extends from northern Saskatchewan toward the south into the Ontario and Québec and then northward toward eastern Newfoundland (Rowe and Sheard, 1981). The Atlantic Maritime (EZ7) includes the Appalachian mountain region, covering 2% of Canada, extends from the mouth of the St. Lawrence River and Bay of Fundy into coastlines of New Brunswick, Nova Scotia, and Prince Edward Island. The Mixedwood Plains (EZ8) is the most southerly ecozone, covering 2% of Canada, but includes the country's most populated regions in Ontario and Québec. The Boreal Plains (EZ9), covering 7% of Canada's landmass in western Canada, from British Columbia to the southeastern corner of Manitoba in the south of Boreal Shield (Ireson et al., 2015). The Prairies (EZ10) extends from south-central Alberta to southeastern Manitoba, covering 5% of

Canada's landmass and the majority of Canada's agricultural lands (Nazemi et al., 2017). The Taiga Cordillera (EZ11) includes 3% of Canada with the least amount of Canada's forest and lies along the northern portion of the Rocky Mountains (Power and Gillis, 2006). The Boreal Cordillera (EZ12) covers 5% of Canada from northern British Columbia to the southern Yukon, with mountainous uplands and forested lowlands. The Pacific Maritime (EZ13) mainly includes the coastal mountains of British Columbia and lands adjacent to the Pacific Coast, having the warmest and wettest climate in the country, in an area around 2% of Canada (Wiken 1986). The Montane Cordillera (EZ14), with the most diverse climate in Canada, includes 5% of Canada in mountainous areas of southern British Columbia and southwestern Alberta and provides headwater flow to some important river systems such as Fraser, Saskatchewan, and Athabasca (Marshall et al., 1999). Finally, Hudson Plains (EZ15) includes 4% of Canada in the southern part of Hudson Bay with a large number of wetlands.

Natural streamflow regimes in Canada have undergone drastic changes in recent years, which are expected to increase under future climate change conditions (Woo et al., 2008). Observed and projected changes in streamflow regimes are not only between different regions (Kang et al., 2016; Islam et al., 2019); but also occur within the same ecological and/or hydrological regions (Whitfield, 2001, 2020). For instance, there are significant differences between forms of change in streamflow regimes between the northern and southern Pacific (Kang et al., 2016; Brahney et al., 2017). Similarly, glacier-fed rivers in northern Canada show increases in summer runoff (Fleming and Clarke, 2003); whereas other rivers show a tendency toward decreasing summer runoff (Fleming and Clarke 2003; Janowicz, 2008, 2011).

To diagnose simultaneous changes in natural streamflow regimes across Canada, we use the data from Reference Hydrometric Basin Network (RHBN; Water Survey of Canada, 2017, http://www.wsc.ec.gc.ca/). RHBN includes 782 Canadian hydrometric stations that measures streamflow at unregulated tributaries and are particularly suitable to address climate change impacts on natural streamflow regimes (Brimley et al., 1999; Harvey et al., 1999). Considering the available data for the period of 1903 to 2015, we search for the largest subset of hydrologically unconnected stations with the longest continuous daily record during a common period and less than a month worth of missing data in a typical year. This results into selecting 105 streamflow stations during the water years of 1966 to 2010 (1 October 1965 to 30 September 2010). Table 2 summarizes the number of selected stations within each ecozone.

Table 2. List of Canadian ecozones with at least one RHBN station in this study, along with their abbreviations and the number of RHBN stations considered within each ecozone.

Abbreviation	Ecozones	# of stations	Abbreviation	Ecozones	# of stations
EZ2	Northern Arctic	1	EZ8	Mixedwood Plains	5
EZ3	Southern Arctic	1	EZ9	Boreal Plains	6
EZ4	Taiga Plains	1	EZ10	Prairies	2
EZ5	Taiga Shield	4	EZ12	Boreal Cordillera	7
EZ6	Boreal Shield	25	EZ13	Pacific Maritime	9
EZ7	Atlantic Maritime	25	EZ14	Montane Cordillera	19

Table S1 to S4 in the Supplement introduce these stations across the four drainage basins in Canada. Figure 5 shows the distribution of the selected stations across the 15 ecozones. As it is clear, the density of selected stations varies greatly among ecozones. The highest numbers of stations are within Atlantic Maritime, Boreal Shield, and Montane Cordillera; while Southern and Northern Arctic as well as Taiga Plains, include only one; and there is no station in the Arctic Cordillera, Taiga Cordillera, and Hudson Plains. Looking however at the drainage basins, the selected stations cover all 14 main Canadian sub-basins – see Table S5 and Fig. S1 in the Supplement.

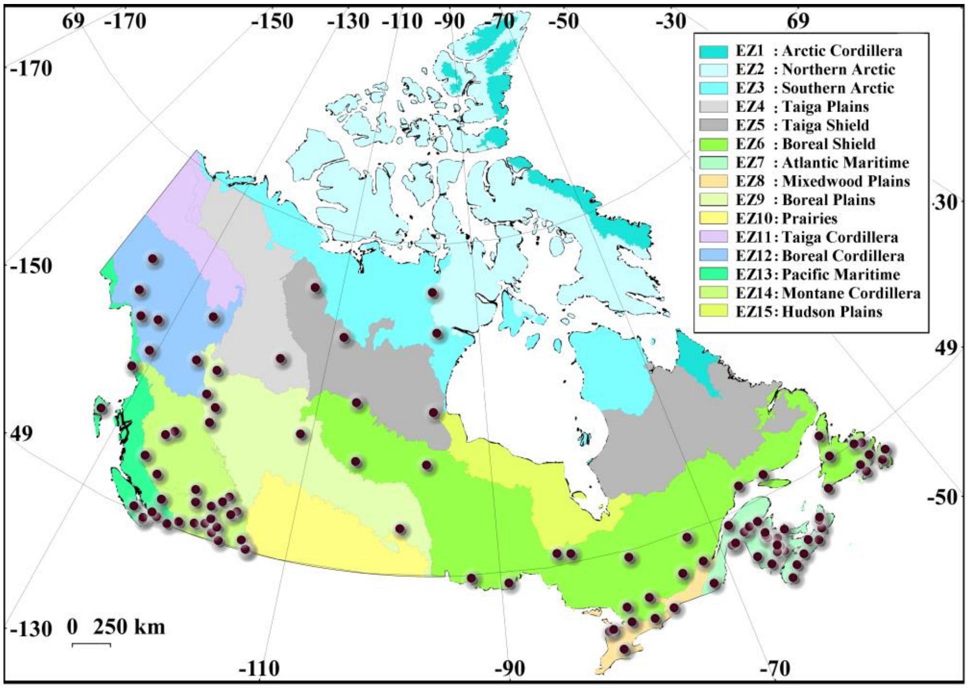

Figure 5 The distribution of the selected 105 RHBN streamflow stations within the Canadian ecozones.

4 Results

We apply the framework proposed in Sect. 2 to the 105 selected RHBN streams. At each stream, we first convert the daily discharge data into runoff depth in millimeters per week and calculate the thirty streamflow features introduced in Table 1. We then consider a multi-year timeframe for clustering and assigning initial membership values. The length of this timeframe should be chosen in a way that (1) provide a notion for streamflow regime, and (2) provide enough timeframes to assess evolution in membership values. As the aim is to address temporal changes in the streamflow regime, the baseline timeframe is considered at the beginning of the streamflow timeseries. Here, we present our result based on considering decadal timeframes and the period of 1966-1975 as the baseline. We address and discuss the sensitivity of our results to these assumptions in Sect. 5.

4.1 Identifying natural streamflow regimes in Canada

We attempt to find the optimal number of clusters empirically from the pool of $c = \{2, 3, \ldots, 10\}$, using the three validity indices introduced in Section 2.3. Figure S2 in the Supplement shows the result of this investigation, revealing the optimal number of clusters as six; because decreasing slopes of the three validity indices flatten after $c = 6$. To provide a sense of these streamflow regimes and their changes in time, we visualize the shapes of annual streamflow hydrographs in the archetype streams during the baseline and the last decadal timeframe (i.e., 1966 to 1975 *vs*. 2001 to 2010) in Figure S3 in the Supplement. Archetype streams are those streams that have the highest association to the identified regime types and can represent the characteristics of a given regime better than other members of the cluster. Table 3 introduces these six regimes along with their notation and archetype streams. We name clusters based on two key characteristics, i.e. the form of hydrologic response (i.e. fast- *vs.* slow-response) as well as the timing of the annual peak flow (i.e., cold-season, freshet, and warm-season peak). The form of hydrologic response can be proxied by variability in the annual streamflow hydrograph. The higher the variability in the annual streamflow hydrograph is, the faster the hydrologic response is.

Table 3. Six identified regime clusters along with their labelled regime type and archetype stream.

Cluster	Regime type	Archetype (representative) stream
C1	slow-response/warm-season peak	Kazan River above Kazan Falls (HYDAT ID: 06LC001)
C2	fast-response/ warm-season peak	Clearwater River near Clearwater Station (HYDAT ID: 08LA001)
C3	slow-response/freshet peak	Matawin River at Saint-Michel-des-Saints (HYDAT ID: 02NF003)
C4	fast-response/freshet peak	Gander River at Big Chute (HYDAT ID: 02YQ001)
C5	slow-response/cold-season peak	Beaver Bank River near Kinsac (HYDAT ID: 01DG003)
C6	fast-response/cold-season peak	Sproat River near Alberni (HYDAT ID: 08HB008)

Figure 6 shows a synoptic look at the distribution of streams belonging to each flow regime during the baseline timeframe across 15 Canadian ecozones. In each panel, the red star represents the archetype stream and streams with membership values of 0.1 and higher are shown with circles. The larger the size of a circle is, the higher the degree of membership to each cluster is. As Fig. 5 shows, the six clusters are geographically identifiable and resemble some of the already-known regime types across the country (see Whitfield, 2001; Bawden et al., 2015; Burn and Whitfield, 2016; Bush and Lemmen, 2019).

The "slow-response/warm-season peak" regime, i.e. cluster C1, includes streams with strong seasonality, high discharge in summer, and lower variability in annual streamflow hydrograph compared to cluster C2, i.e. "fast-response/warm-season peak" regime. Cluster C1 is characterized by a gradual rise after spring snowmelt, prolonged peak discharge throughout summer, gradual recession during fall, and low runoff in winter (Déry et al., 2009). Streams belonging to C1 spread mostly in northwestern Canada and are either glacial-fed or lake-dominated streams. The Kazan River releasing into the Baker Lake in Nunavut is the archetype stream for this regime type. C2 is very similar to C1, however with relatively higher variations in annual streamflow hydrographs. The stream belonging to this stream are mainly concentrated in western Canada, particularly in Montane Cordillera (46% of streams), and include streams that are fed mainly through snow and glacial melts (Eaton and

Moore, 2010; Moore et al., 2012; Schnorbus et al., 2014). There are, however, streams belonging to C2 that are located in Boreal Shield (23% of streams), where the streamflow generation is governed by other processes such as fill and spill (Spence and Phillips, 2015). The Clearwater River near Clearwater in southern Alberta is the representative stream for this regime type.

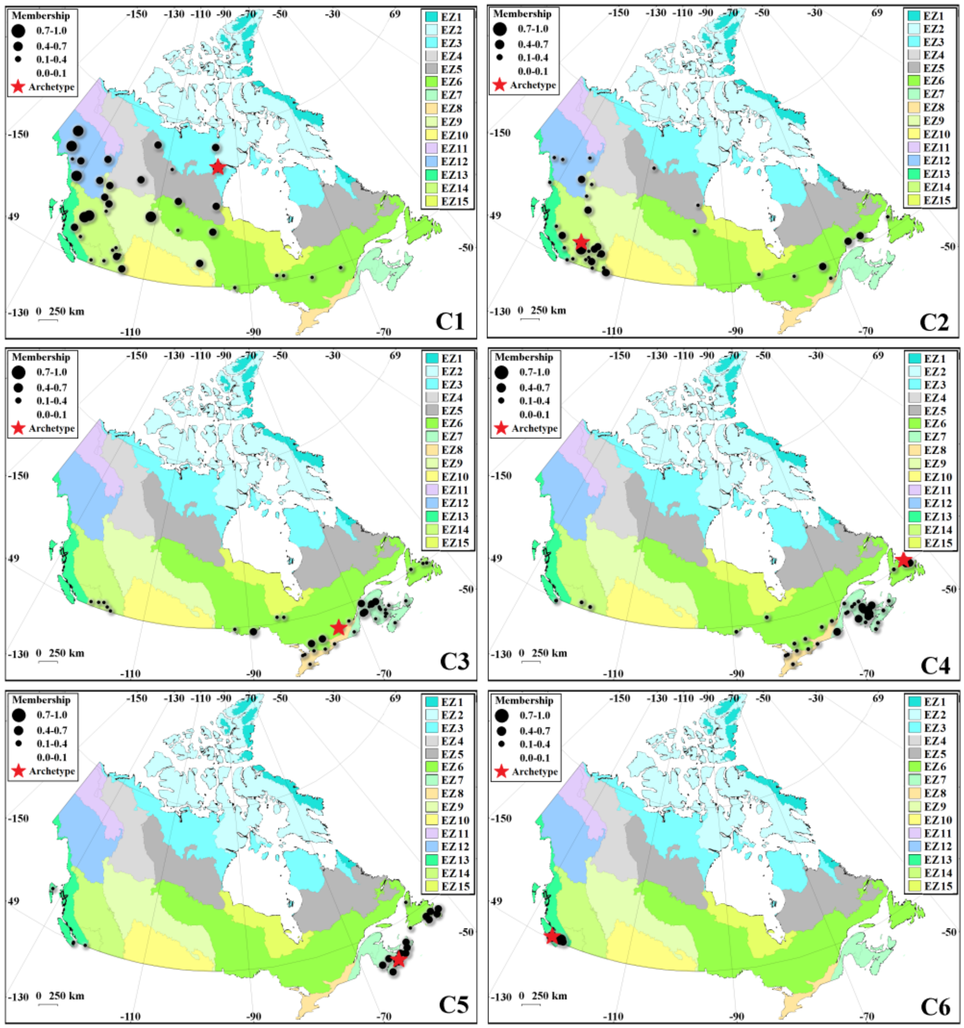

Figure 6. The distribution of the identified regime types across Canadian ecozones during the baseline 1 timeframe of 1966 to 1975. Each stream is represented by a circle with a radius proportional to a membership degree quantifying the association to a given regime type. Only RHBN stations with degrees of membership of 0.1 or higher are shown in each panel. The red stars are the archetype stations related to each regime type.

The cluster C3, i.e. the “slow-response/freshet peak” regime, includes streams in which the annual streamflow volume is mainly contributed by a short high flow period during spring snowmelt, sharp recession in summer, with relatively lower variations in the shape of hydrograph compared to the cluster C4, i.e. “fast-response/freshet peak” regime. Nearly 45% of the streams with this regime type are located in Atlantic Maritime. The rest are distributed in Boreal Shield (28%), Mixedwood Plains (15%), and Montane Cordillera (12%). The Matawin River originated from the lake Matawin in Québec is the archetype for the C3 regime. The streams belonging to C4 are also dominated by spring snowmelt but showing more variation in the shape of annual hydrographs compared to the C3 regime. Streams belonging to the C4 regime often have two distinct peaks, one in spring induced by snowmelt and one in fall due to high precipitation; and from that sense, they largely resemble nivo-pluvial streams (Hock et al., 2005).

Almost all streams belonging to the C4 regime are located in eastern Canada (50% in Atlantic Maritime, 26% in Boreal Shield, 16% in Mixedwood Plains). Gander River at Partridgeberry Hill in Newfoundland is the archetype for this regime. The cluster C5, i.e. "slow-response/cold-season peak" regime, comprises streams with weak seasonality and slightly more discharge in fall and winter. The annual flow for streams belonging to this regime is more influenced by rainfall around later fall, followed by a slight increase in discharge due to snowmelt; and therefore, they resemble a hybrid pluvio-nival regime (Kang et al., 2016). The concentration of streams belonging to this regime is again in the eastern Canada (48% in Atlantic Maritime; 33% in Boreal Shield), with few streams being in the Pacific Maritime. Beaver Bank River in Nova Scotia is the representative stream for this regime type. Finally, the cluster C6, i.e. "fast-response/cold season peak regime, is similar to the C5 regime and exhibits a weak seasonality, but with a higher variation in shapes of annual hydrographs. The runoff in streams belonging to this regime is dominated by heavy precipitation, especially during winter, and lower runoff during summer, which resembles the pluvial regime (Wade et al., 2001; Whitfield, 2001). Streams belonging to this regime are only concentrated in the Pacific. The Sproat River near Alberni is the archetype stream of the C6 cluster.

4.2 Detection of changing streamflow regimes

To understand temporal shifts in streamflow regimes throughout selected RHBN streams, we calculate the decadal membership values as shown in Fig. 2. We accordingly apply the Mann-Kendall trend test with the Sen's Slope on the time series of decadal memberships. The detailed results including the membership timeseries for all streams and corresponding trend analyses are shown in Figs. S4 and S5 in the Supplement over major drainage basins/sub-basins as well as the terrestrial ecozones in Canada, respectively. Figure 7 summarizes our findings over the 15 Canadian ecozones. The color (blue *vs.* red) and the size (large *vs.* small) of triangles show decreasing *vs.* increasing trends as well as significant *vs.* insignificant trends at p-value ≤ 0.05. Although inconsistent patterns of change are observed in Boreal and Montane Cordillera, particularly between the southern and northern regions, there are clear downward trends in the belongingness to regime C1 in Taiga Shield and Boreal Shield. Upward trends are observed in membership values of C2 in Boreal Cordillera and Taiga Shield, while downward trends are seen in the belongingness to C2 in southern and eastern parts of Montane Cordillera and Boreal Shield. The C3 regime shows intensification in Montane Cordillera and Boreal Shield. It also intensifies in southern parts of Atlantic Maritime but weakens in northern regions. The pattern of change in C4 is very similar to C3, but with less significant downward trends in northern parts of Atlantic Maritime. Considering the C5 regime, streams mainly show decreasing trends in the Appalachian region including eastern Boreal Shield, and southern parts of Atlantic Maritime. Mixed patterns of change in membership degree are observed in the Pacific Maritime for both C5 and C6 regimes.

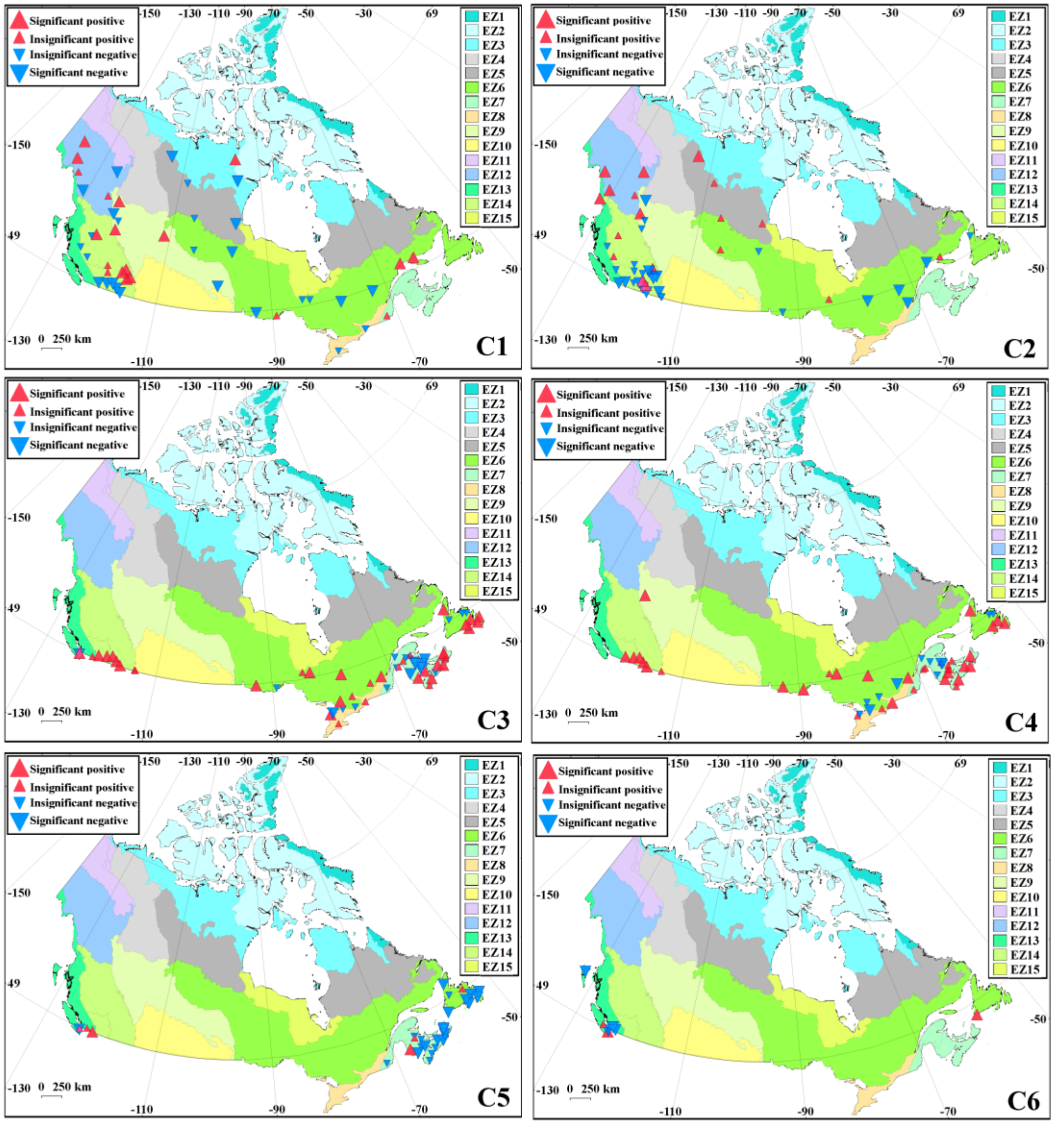

Figure 7. Trends in decadal memberships, quantifying the change in association of the 105 selected RHBN streams to the six regime types during 1966 to 2010.

The analysis of trends in memberships shown in Fig. 7 sets the scene for investigating regime shifts throughout the country by quantifying the rate of relative shift between opposing significant trends. Figure S6 in the Supplement summarizes the results. Overall, the dominant modes of transition at the ecozone scale are from C1 to C2 in the northern ecozones (EZ5 and EZ12), from C2 to C1 and from C2 to C3 in the western ecozones (EZ9 and EZ14), from C2 to C3 in the two stations located in the Prairies, from C1 to C3 in the eastern ecozones (EZ6, EZ8, and EZ15), and from C5 to C4 in the Appalachian region (EZ7 and eastern part of EZ6). The variability between the regime shifts inside each ecozone can be described by elevation. To better synthesize the findings in Canada and highlight dominant regime shifts and their geographic extent across the country, Fig. 8 shows Sankey diagrams, demonstrating how initial regime types in the considered streams, grouped by the ecozones in the left side of each panel), transform to one particular target regime type (right side in each panel). The six natural regime types are distinguished by color codes and stations within each ecozone are sorted from the lowest to the highest elevation from top to the bottom. The width of each arrow is proportional to the rates of shift, calculated using Eq. 7. The highest rate of a shift in each stream and/or ecozone can be considered as the dominant regime shift.

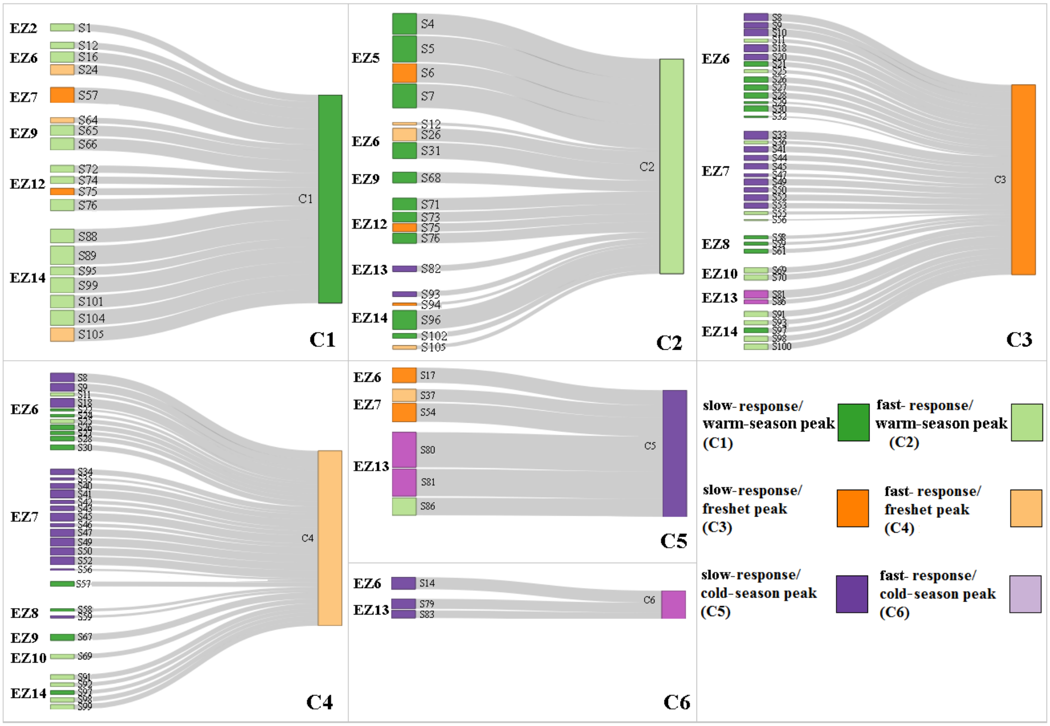

Figure 8. Sankey diagrams showing transitions in Canadian natural streamflow regimes described across ecozones from 1966 to 2010. Each panel reveals transformation from five potential regime types to one particular target regime. Streams in the left side are grouped according to ecozones and are sorted from the lowest to highest elevations from the top to the bottom. Colors show the six regime types. The widths of arrows are proportional to the rate of shift.

Some important findings with regard to forms of regime shifts across Canada can be made from Fig. 8. First and foremost, while regime shifts are vibrant, there are some dominant regime shifts that are frequently observed across different ecozones. For example, frequent shifts are observed from C2 to C1 as well as C1 to C2 that are quite strong across Montane Cordillera and Taiga Shield, respectively. Second, it is possible that the streamflow regime in a given ecozone shifts from one regime to two or more regime types. For instance, streamflow in Atlantic Maritime shifts from C5 to C3 and C4. Also, it is possible to have opposing regime shifts in a given ecozone. As an example, the flow regime varies from C5 to C6 and vice versa across Pacific Maritime. Such variabilities in regime shift can be partially explained by latitude. More generally, it is possible to shift from two or more regime types into one or more regime types across a particular ecozone. For example, streams with C1 and C5 regimes are shifting to C3 and C4 across Boreal Shield. Such variabilities within an ecozone can be described in many cases by elevation. In Boreal Shield, for example, elevation controls the constitution of the initial streamflow regime from C5 in lowlands to C1 in highlands. Finally, the most frequent regime shifts are not necessarily the strongest ones. For instance, the streamflow regime shifts across 6 ecozones toward C3 and C4 but the rates of the shift are not strong when compared with the shift between C6 to C5 that happens in limited streams in Pacific Maritime.

4.3 Identifying forms of transformation in streamflow regimes

The procedure presented in Sect. 2.5 attributes regime shifts to changes in streamflow characteristics using dependence analysis. Figure 9 summarizes the results of attribution in the 105 RHBN stations. Streams are shown in rows, grouped in each ecozone, and sorted from low to high elevations from the top to the bottom. For each stream, there are three groups of cells, with 15, 15, and 2 cells from left to right respectively. The first two groups of cells are related to the values of mean and variance for the 15 considered IHAs, respectively – see Table 1 for the definition of 30 features considered. In these two groups of cells, shades of blue and red show negative and positive dependencies between a given pair of streamflow characteristic and membership degree, respectively. Note that we only identify those streamflow characteristics that have significant dependencies with variations in membership degrees based on Kendall's tau (p-value ≤ 0.05) Color saturations show the values for the coefficient of determination, quantifying the percentage of variability in membership degrees that are described by the variability in streamflow characteristics. The last two cells are related to the dominant regime shift in each stream from one initial regime (second cell from right) to an altered regime (first cell from the right). The color scheme, defining the regime types, is shown in the legend. The analyses over basin and sub-basin scales are presented in Figs. S7 and S8 in the supplement.

The most important observation is the fact that in more than 80% the considered natural streams, there are some identifiable regime shifts that are significantly dependent on the changes in the streamflow characteristics. Some dominant regime shifts are frequent within an ecozone, while some are less frequent and may depend on latitude and/or elevation. In the only considered stream in the Northern Arctic, the shift from the C2 to the C1 regime is attributed to the earlier and more variable timing of the annual low flow, and the increasing June flow. An opposing shift is observed in Taiga Shield, i.e. from C1 to C2, which can be attributed to the earlier and more variable timing of annual high flow, and the increasing seasonal flow in fall. The regime shift from C5 to C4 in the lowlands of Boreal Shield is attributed to the decreasing mean and variance of annual flow particularly in August. In the highland of this ecozone, however, the dominant regime shift is from C1 to C3 and can be attributed to the decreasing monthly flow in August and September, and more variability in the timing of the annual low flow. In Atlantic Maritime, particularly across lowlands, decreasing mean and variation of the flow in August along with decreasing monthly flow in June and July, and decreasing mean annual and seasonal flow in the fall lead to a shift from C5 to the C4.

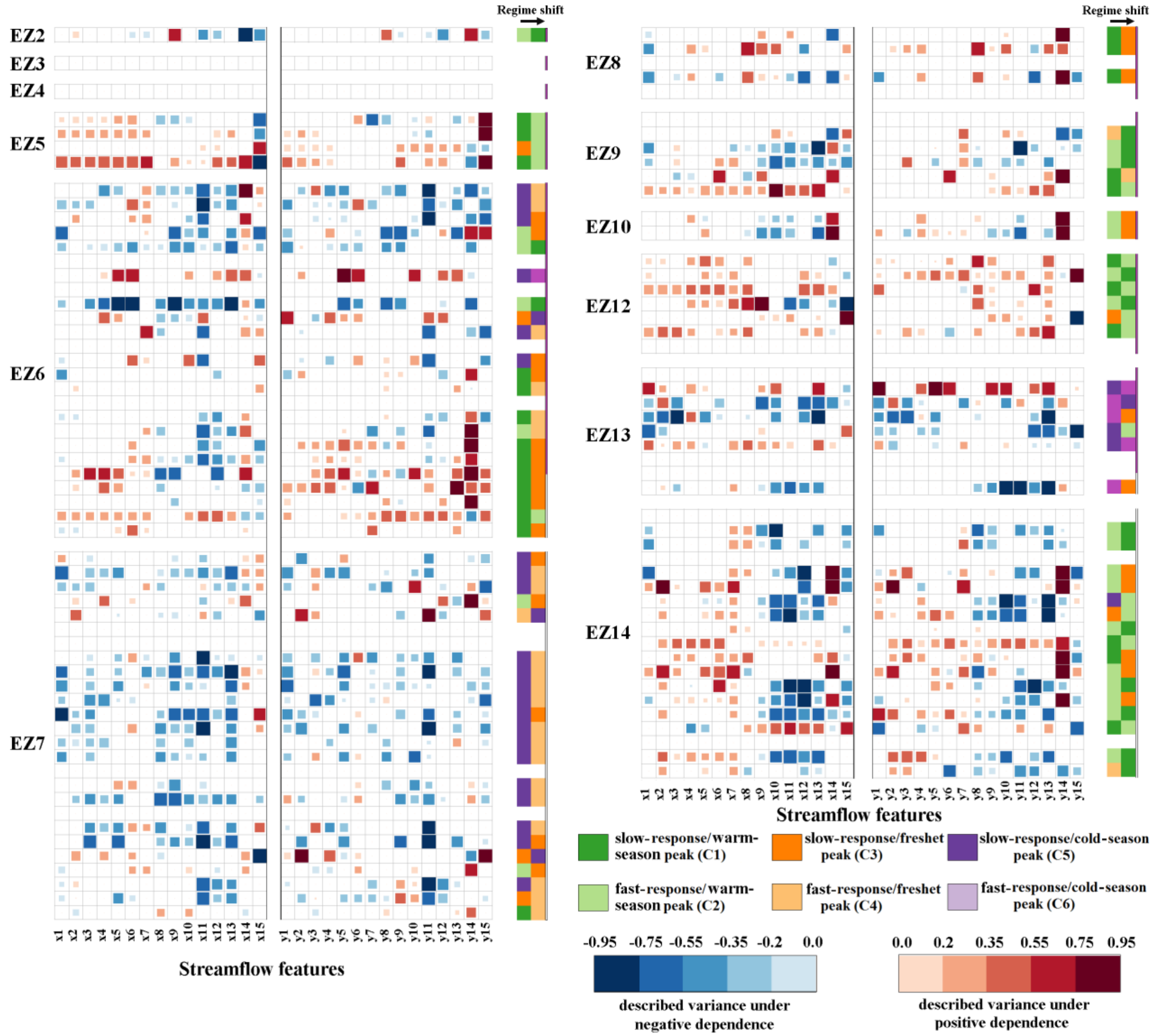

Figure 9. Dominant regime shifts across 105 RHBN streams in Canada attributed to the first and second moments of the 15 IHAs considered. Shades of red and blue show the positive and negative dependencies between changes in NSFs and degrees of membership, respectively. Color saturations are proportional to the values of coefficient of determination. The dominant regime shift at each stream is identified by the color scheme described in the legend. Streams are grouped in ecozones and sorted from low (top) to the high (bottom) elevations

In Mixedwood Plains, the shift from C1 to C3 is attributed mainly to earlier and more variable timing of annual low flow. In the lowlands of Boreal Plains, the increasing variation in April’s flow, and decreasing annual and summer flows contribute to the shift from C2 to C1. Streams in the highlands of Boreal Plains, however, shift from C1 to C2 due to the increasing annual and summer flows, along with later and more variable timing of low flows. In Prairies, in the two considered streams, the shift from C2 to C3 is attributed to delayed and more variable timing of low flows and decreasing summer flows. In Boreal

Cordillera, more variable annual flow and increasing mean and variation in May flow correspond to the shift from C1 to C2. Opposing shifts from C2 to C1, however, are mainly attributed to the increasing monthly flows in February, March, April, and May. The most pronounced shift in Pacific Maritime is from the C5 to C6, which mainly corresponds to increasing mean and variation of October flow, and increasing annual flows. The most pronounced shift in Montane Cordillera is from C2 to C1 for the streams in the northern part, attributed to decreasing mean and variability in July flow and increasing monthly flow in April and May. Streams in southern parts, however, shift from C2 to C3, attributed mainly to increasing monthly flow in February, March, and April, more variability in the timing of the low flow as well as decreasing September flow.

5 Discussion

The application of the proposed methodology in Canada reveals six distinct natural regimes across the country, address their change in time and space, attribute dominant regime shifts to changes in a range of streamflow characteristics at each stream and accordingly upscale the findings from individual streams to ecozones. Having said that, still there are some unanswered questions. First, it is still unclear how robust our proposed algorithm is particularly in light of the assumptions made with respect to the length of the timeframes and/or selecting the baseline period. Second, it is obvious that our selected streams are only a sample of available RHBN stations across Canada and it is still unclear how our findings can be extended to unseen streams. Finally, there is a large body of literature, reporting shifts in streamflow regimes across different regions in Canada due to changes in temperature patterns, magnitude and form of precipitation, snowmelt and snow accumulation processes as well as glacier retreat and permafrost degradation. As a result, it is crucial to frame and position our findings with respect to earlier studies. These three tasks are pursued in this section.

5.1 Addressing uncertainty

The results presented in Sect. 4 are based on considering decadal timeframes and choosing the first decadal timeframe as the baseline period. Here we relax these two assumptions and monitor alterations in our findings. First, we repeat the clustering algorithm over all possible decadal timeframes throughout the study period and recalculate the cluster centers. This experiment addresses the sensitivity of our clustering algorithms to the choice of baseline period. Second, we repeat the approach implemented in Sect. 4 again with considering 15- and 20-year timeframes and address how cluster centers, as well as our specific findings would alter by increasing the length of timeframe. We do not consider timeframes less than decadal length due to the insufficiency for trend analysis. We also do not consider timeframes larger than 20 year to allow two fully independent timeframes during the study period with a few years gap. Figure 10 summarizes our findings in terms of the sensitivity of our clustering results with respect to the two assumptions made. Panel (a) shows the cluster centers when different decadal baselines are considered. Colored dots show the centers of clusters related to all possible decadal timeframes expect the period of 1966-1975 that are scaled into two dimensions using the Multidimensional Scaling (MDS; Cox and Cox, 2008).

Black crosses show the centers of the first decadal timeframe mapped using the MDS. Colors identify regime types. The result clearly shows that despite changing the baseline timeframe, the distinction between cluster centers are maintained and the position of centers does not substantially change by changing the baseline period. Panel (b) shows the results of our sensitivity analysis with respect to changing the length of timeframe. Again, there are not significant changes in the cluster centers. These two findings highlight the robustness of our clustering analysis.

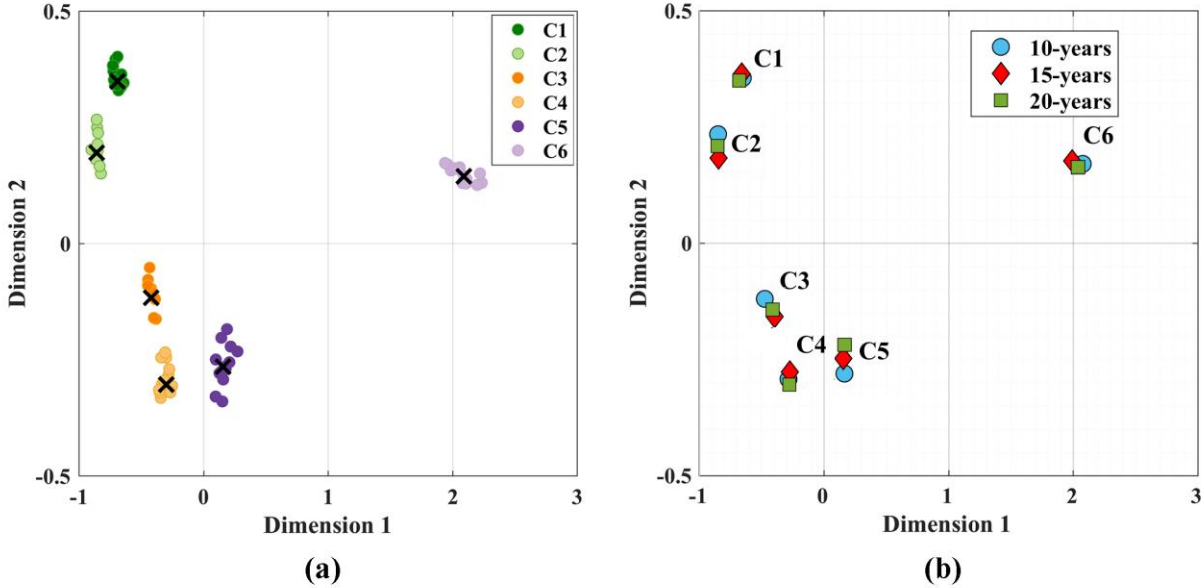

Figure 10. The sensitivity of the cluster centers to (a) the choice of decadal timeframe for clustering, and (b) the length of the timeframe used for analysis. In panel (a) dots show the two dimensional scaling of the cluster centers based on the relative distance of cluster centers from one another. Black crosses show the centers identified by choosing the first decadal timeframe. Panel (b) shows the two dimensional scaling of the cluster centers considering 10-, 15- and 20-year timeframes.

We also look at possible differences in the direction of trends in membership degrees, dominant regime shifts, as well as the attribution to streamflow features at the basin scale, if the length of timeframes are changed. Figure 11 (left column) intercompares the results obtained by 10-, 15- and 20-year timeframes in terms of percentages of similarities in the direction of trends during 1966 to 2010 at each basin. In brief, there are at least 80% agreements between the results obtained in the Pacific and the Arctic basins. There are more discrepancies in the direction of trends in the Atlantic and Hudson Bay basins. This is particularly the case for the C1 regime in the Hudson Bay and for the C3 and C4 regimes in the Atlantic, for which the results are less consistent among different timeframes; yet, in the worst-case scenario (i.e., the C4 regime in Atlantic), there is still more than 60% agreement between the results of trend analysis obtained by 10-, 15- and 20-year timeframes.

Dominant regime shifts are also performed with 15- and 20-year timeframes and are intercompared with corresponding results obtained by decadal timeframes. Our analysis shows that results obtained by 15- and 20-year timeframes are in large agreements with the results obtained using decadal timeframes. Even for the case with the largest discrepancy (i.e., C4 regime in the Atlantic), there is 86% agreement in terms of the direction of shift in streamflow regimes, obtained by 10- and 20-year timeframes. In terms of attribution of regime shifts to changes in streamflow characteristics, again the results obtained by different lengths are in large agreement in at least 80% of streams.

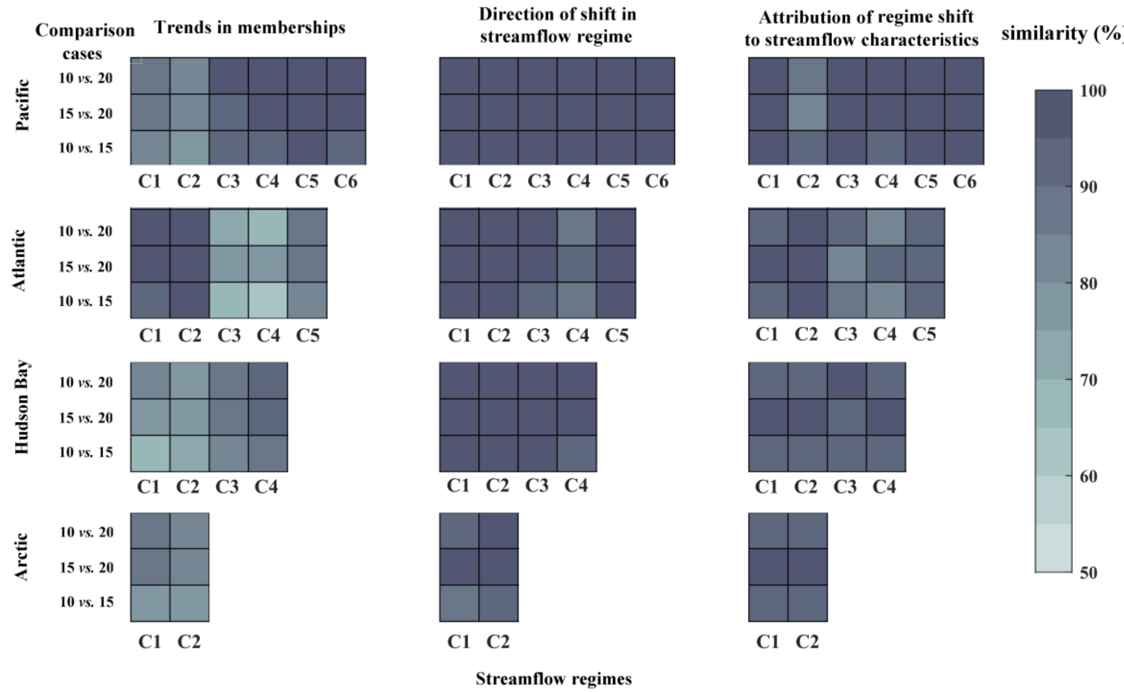

Figure 11. Similarities (in percentage) between the results obtained by 10-, 15- and 20-year timeframes related to trends in membership values, direction of shift in streamflow regimes, and attribution to streamflow characteristics in the four major Canadian basins.

5.2 Validation in unseen streams

One important question remained unanswered is how the six regime types identified can be extended into out-of-sample streams. Here we investigate this in the Prairies ecozone, a region with importance for global food security. Natural streams in Prairies have been relatively overlooked in the literature (Whitfield et al., 2020), because the majority of annual streamflow volume is contributed from mountainous headwaters outside of Prairies and the fact that large proportion of the land does not contribute into the streamflow. In addition, only two stations in Prairies meet our data criteria in Sect. 3. Here, we reduce the length of data and investigate for new streams that satisfy our data criteria during 1976 to 2010. This has resulted into selection of nine new stations – see Fig. 12 for the location of these stations (P1 to P9). The detailed information about these stations are provided in Table S6 in the Supplement. Here we investigate how these new stations fit in previously identified regime types, check the trends in the membership degrees, and identify dominant regime shifts in these streams. We compare our findings in the nine new stations with the two previously selected stations in the Prairie region, namely, Waterton River near

Waterton Park (S69) and Belly River near Mountain View (S70) during the common period of 1976-2010 for which the nine new stations are selected. The right panel shows the analysis of trends in anomalies of decadal memberships, in which stations are sorted from the east to west from the top to the bottom. The analysis of trends in membership degrees shows mainly decreasing trends for C1 and C2 regimes and increasing trends for C5 and C6 regimes. Regarding C3 and C4 regimes, mainly upward trends are observed in the east; whereas, downward trends are observed in the west. These findings are in line with our results in S69 and S70. The two columns at the right side of right panel are related to the dominant regime shift in each stream. The legend demonstrates the six identified regime types. Although the regime shifts are vibrant, the dominant regime shift observed is from C2 to C5, which is the same in S69 and S70 during the period of 1976-2010.

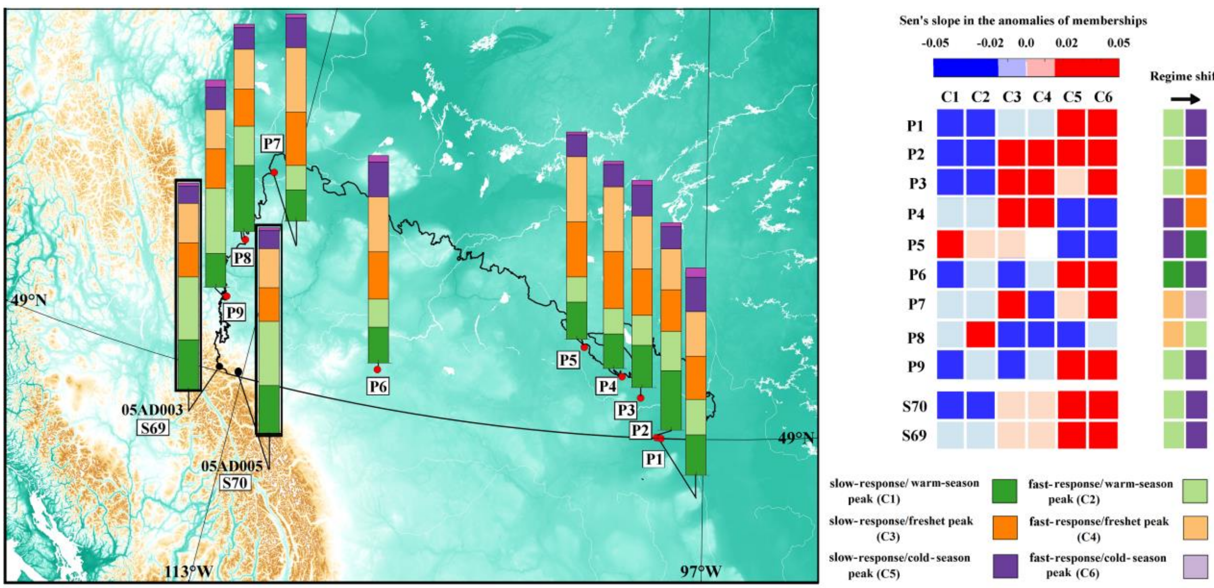

Figure 12. Validation of the proposed algorithm in nine unseen streams in the Canadian Prairies using nine unseen during 1976 to 2010. The color bars in the left map show the degrees of membership to each cluster. The right panel shows the trends in the degree of membership in the six clusters in the considered 11 stations. Positive and negative trends are shown with red and blue colors, respectively. Sharp colors show significant cases. Unseen stations S1 to S9 are sorted from east to west from the top to the bottom.

5.3 Summary of findings and positioning against earlier studies

Although to the best of our knowledge, our work is the first study in which a fully algorithmic framework is used to provide a temporally homogeneous view on recent changes in pan-Canadian streamflow regime; the literature of Canadian hydrology is rich in terms of documenting changes in streamflow characteristics across the country. Thanks to pioneering works of so many hydrologists before us, including the late iconic northern hydrologist, Richard Janowicz, to whom this paper is dedicated. Here we attempt to position our results with respect to earlier studies. Table 4 summarizes our findings in terms of dominant regime shifts and associated changes in streamflow characteristics at the sub-basin scale.

Table 4. Positioning our finding with respect to earlier studies across major Canadian basins and sub-basins

Basin	Sub-basin (stream location)	Dominant regime shifts	Earlier findings on changes in streamflow characteristics (reconfirmed in this study)	New findings on changes in streamflow characteristics (discovered exclusively in this study)
Pacific	Yukon	C3 to C1	Earlier timing of low and high flows; higher variability in timing of high flows (Burn 2008; Brabets and Walvoord, 2009; St. Jacques and Sauchyn, 2009)	Increasing flow in September; increasing flow variability in April and May
	Seaboard (north)	C1 to C2	Increasing winter flows (Déry et al., 2009)	Increasing monthly flow in May; earlier timing of low flow; increasing variability in March, May and annual flows
	Seaboard (south)	C1 to C3	Decreasing annual and monthly flow from April to June; decreasing flow in fall (Déry et al., 2009; Pike et al., 2010)	Delayed and more variable timing of annual low flow; increasing variability in February's monthly flow
	Fraser (north)	Case 1: C1 to C2 Case 2: C2 to C1	No earlier study in this region was found.	Case 1: Increasing mean and variance in annual and summer flows; increasing monthly flows in May and June; increasing variation in timing of low flow and the quantity of spring flows. Case 2: Decreasing mean and variance of annual flow; decreasing monthly flows in July and October; earlier timing of high flow; decreasing variability of monthly flows in May, August, September
	Fraser (south)	C2 to C5	Decreasing summer flows (Stahl and Moore, 2006); Increasing variability in monthly flows in November and April (Déry et al., 2012; Thorne and Woo, 2011)	Earlier timing of high flows; increasing mean monthly flows in November and April
	Columbia (north)	C2 to C1	Decreasing annual and summer flows (Stahl and Moore, 2006; Fleming and Weber, 2012; Forbes et al., 2019)	Decreasing variability in annual flow, and monthly flows of August and September
	Columbia (south)	C1 to C3	Increasing flow in April and decreasing flow in September (Whitfield and Cannon; 2000; Whitfield, 2001); Earlier timing of high flow (Burn and Whitfield, 2016; Burn et al., 2016)	Delayed timing and higher variability of the annual low flow; increasing mean and variance of flow in November's flow
Atlantic	Seaboard (north)	C5 to C3	increasing spring flows, corresponding to increased snow precipitation (Thistle and Caissie, 2013)	Increasing monthly flow in April; decreasing monthly flow in June; delayed and less variable timing of low flows; less variation in annual timing of high flows; decreasing mean and variation of monthly flow in August
	Seaboard (south)	Case 1: C5 to C4 Case 2: C3 to C5	Case 1: decline in the annual flow (Whitfield and Cannon, 2000; Yue et al., 2003; Thistle and Caissie (2013) Case 2: decline in winter flows, probably due to positive AMO (Whitfield and Cannon, 2000; Assani et al., 2012)	Case 1: Decreasing monthly flow in May, June and August; increasing monhly flow in March; Decreasing variability in February's monthly flow Case 2: Decreasing monthly flow in May and June; later timing of low flows
	St. Lawrence (north)	C3 to C1	lower variations in timing of low flow (Thistle and Caissie, 2013)	Decreasing annual flow as well as seasonal flows in summer and winter; decreasing monthly flows in June, less variation in monthly flows of February, May, June
	St. Lawrence (south)	C1 to C3	No earlier study in this region was found.	Increasing mean and variation in monthly May flows; decreasing mean and variation in September flows; decreasing flow in October, increasing flow in February; increasing variance in timing of low flows; increasing variability in January's monthly flows
	Saint John- St. Croix	C5 to C4	Decreasing monthly flow in May (Kingston et al., 2011)	Decreasing annual flow; deceasing monthly flows in February and June; decreasing mean and variability of monthly flows in October and August
Arctic	Seaboard	C1 to C2	Earlier and more variable timing of high flows; increasing winter flows (Burn, 2008; Déry et al. 2016); earlier timing of high flows (Yang et al.; 2015)	increasing mean and variability of seasonal flow in fall, heightened variability in monthly flow in June
	Lower Mackenzie	C1 to C2	Increasing annual and winter flows (Smith et al., 2007; Walvoord and Striegl, 2007; St. Jacques and Sauchyn, 2009; Rood et al., 2016)	Increasing annual and seasonal flows during fall; increasing June's monthly flow; heightening variability in the timing of high flows
	Peace Athabasca	C2 to C1	Decreasing monthly flow in July (Yang et al., 2015)	earlier and less variable timing of low flows
Hudson Bay	Western & Northern Hudson Bay	C1 to C3	Increasing winter flows; decreasing summer flows; increasing variability in winter flows (Déry et al., 2011, 2018)	Delayed and more variable timing of low flows; increasing variability in February's monthly flow
	Northern Quebec & Ontario	C1 to C2	Increasing annual and winter flows, increasing variability in timing of high flows	Increasing annual and seasonal fall and summer flows; decreasing and less variable monthly flows in May; decreasing monthly flow in June
	Nelson	C1 to C3	Decreasing summer and fall flows Rood et al. (2008); Decreasing summer flows; increasing variability fall and spring flows (Déry et al., 2011)	Decreasing monthly flow in May and June; increasing variability of timing of low and high flows; increasing annual flow and seasonal flows in summer and winter

Table 4 makes a clear distinction between the earlier findings, and those exclusively found in our study. Even though earlier studies have different data periods, and may include streams that are not within the RHBN streams, our study reconfirms previous findings and also reveals new changes in streamflow characteristics that have remained previously overlooked. Our study clearly shows that changes in variability of monthly, seasonal, and annual flows can be important drivers of shift in streamflow regime across the majority of sub-basins in Canada. This is another line of evidence for the complex and multifaceted nature of change in streamflow regime, and the need for a simultaneous look at alterations in both expected values and variability of streamflow characteristics to diagnose changes in natural streamflow regime.

6 Concluding remarks and outlook

This study presents an attempt toward providing a generic algorithm for identifying changing streamflow regimes with global relevance. The proposed approach is based on two fundamental considerations. First, we recognize that streamflow regime is collectively formed by a large number of streamflow characteristics. Second, we acknowledge that streamflow types are rather in the form of spectrums, not clear-cut states; and if regime shifts are caused by climate change, the transition from one regime type to another should be gradual rather than abrupt. To accommodate these two considerations, we suggest representing streamflow regime types as intersecting fuzzy sets, in a way that the belongingness of each stream to each regime type can be quantified by a membership function. Accordingly, monitoring the trends in membership values in time and space can provide a basis to identify the regime shift from one type to another. We consider the existence of a significant trend in membership values as an evidence for the regime shift. In addition, analyzing the covariance of membership values with streamflow characteristics can lay down a basis to attribute the regime shift to alterations in certain streamflow characteristics in time and/or space. A significant dependence between a given regime shift and simultaneous alterations in streamflow characteristics highlights attribution, which can be communicated by R^2.

To apply this algorithm, we consider 45-year of daily data from 105 RHBN streamflow gauges across Canada, to provide a comprehensive and temporally homogeneous look at forms and extents of change in natural streamflow regime in Canada, coast to coast to coast. Our results show that streamflow regime in Canada can be categorized into six distinct regime types with clear physical and geographical interpretations. Analyses of trends in membership values show that alterations in natural streamflow regime are vibrant and can be different across different regions. Overall, in more than 80% of the considered stream there is a dominant regime shift that can be attributed to changes in streamflow characteristics. At the ecozone scale, the dominant regime shifts are from C1 to C2 in the northern ecozones (EZ5 and EZ12), from C2 to C1 and from C2 to C3 in the western ecozones (EZ9 and EZ14), from C2 to C3 in the two stations located in the Prairies, from C1 to C3 in the eastern ecozones (EZ6, EZ8, and EZ15), and from C5 to C4 in the Appalachian region (EZ7 and eastern part of EZ6). The variability between the regime shifts inside each ecozone can be described by elevation and/or latitude. At the basin scale, dominant modes of transition are from C3 to C1 in the northern Pacific and from C1 to C3 in the southern Pacific, between the C4 and C5 regime as well as the C3 and C5 in the Atlantic, between the C1 and C2 in the Arctic, and between C1 and C3 as well as the C2 and C3 regimes in Hudson Bay. The details of change in streamflow regime, however, are subject to a spatial variability within each drainage basin. In Atlantic and Pacific regions, there are clear divides between dominant regime shifts in northern and southern regions. For instance, In the Pacific, the association to C1 is increasing in Yukon and northern parts of Columbia and Fraser sub-basins; but it is significantly decreasing in the southern regions. This can be due to different manifestations of climate change, which are more revealed as temperature increases in the north, and growing ratios of rain over precipitation in south, shifting the streamflow more toward rain-dominated regimes (Fleming and Clarke, 2003). This reconfirms the important role of landscape in regulating the streamflow response to climate change.

The proposed framework provides an opportunity to identify the changing streamflow regimes and attributes such changes to a large set of streamflow characteristics. This approach, however, do not explore the attribution of the shifts in streamflow regimes to the changes in temperature pattern, form and magnitude of precipitation, snowmelt, glacial retreat and permafrost degradation. These can be potential areas for future research. We hope our study triggers more attention to multifaceted nature of change in streamflow regime in Canada and the rest of the world during the current "*Anthropocene*".

Data availability. The analysis is based on data provided by the Reference Hydrometric Basins Network (RHBN) of Environment Canada. The dataset can be accessible through streamflow records of HYDAT, complied by Water Survey of Canada, http://www.ec.gc.ca/rhc-wsc/default.asp?lang=En&n=9018B5EC-1).

Supplement. The supplement related to this article is available online.

Author contributions. MZ, AN and SH designed the methodology; MZ, SH and JS developed the computational procedure; MZ, SH and AN executed the numerical work and analyzed the results; MZ, AN developed manuscript outline and flow; MZ and SH developed the artworks; MZ performed the literature review and wrote the first draft; AN, SH and JS commented and revised the paper; AN and MZ finalized the manuscript.

Competing interests. The authors declare that they have no conflict of interest.

Acknowledgement and dedication. Financial support for this study is provided by Canada Natural Science and Engineering Research Council through Discovery Grant Program, as well as Concordia University through various internal sources. We greatly acknowledge valuable inputs from Elmira Hassanzadeh of Polytechnique Montréal, on the earlier version of this paper. This study is conducted with love and sweat, and is dedicated to the memory of Richard Janowicz, the iconic northern hydrologist who made fundamental discoveries on recent changes in natural streamflow regime in the Great White North: Canadian Hydrology will never forget you, *Rick*.

References

Aksamit, N. O., and Whitfield, P. H.: Examining the pluvial to nival river regime spectrum using nonlinear methods: Minimum delay embedding dimension. Journal of Hydrology, 572, 851-868, https://doi.org/10.1016/j.jhydrol.2019.03.058, 2019.

Amir Jabbari, A., and Nazemi, A.: Alterations in Canadian Hydropower Production Potential Due to Continuation of Historical Trends in Climate Variables. Resources, 8(4), 163, https://doi.org/10.3390/resources8040163, 2019.

Arheimer, B., and Lindström, G.: Climate impact on floods: Changes in high flows in Sweden in the past and the future (1911–2100). Hydrology and Earth System Sciences, 19, 771–784, https://doi.org/10.5194/hess-19-771-201, 2015.

Arnell, N.W. and Gosling, S.N.: The impacts of climate change on river flow regimes at the global scale. Journal of Hydrology, 486, pp.351-364. https://doi.org/10.1016/j.jhydrol.2013.02.010, 2013.

Asadieh, B., and Krakauer, N. Y.: Global change in streamflow extremes under climate change over the 21st century. Hydrology and Earth System Sciences, 21(11), 5863-5874, https://doi.org/10.5194/hess-21-5863-2017, 2017.

Assani, A. A., Landry, R., and Laurencelle, M.: Comparison of interannual variability modes and trends of seasonal precipitation and streamflow in southern Québec (Canada). River research and applications, 28(10), 1740-1752, https://doi.org/10.1002/rra.1544, 2012.

Barnett, T. P., Adam, J. C., and Lettenmaier, D. P.: Potential impacts of a warming climate on water availability in snow-dominated regions. Nature, 438(7066), 303, https://doi.org/10.1038/nature04141, 2005.

Bawden, A. J., Burn, D. H., and Prowse, T. D.: Recent changes in patterns of western Canadian river flow and association with climatic drivers. Hydrology Research, 46(4), 551-565, https://doi.org/10.2166/nh.2014.032, 2015.

Bensaid, A.M., Hall, L.O., Bezdek, J.C., Clarke, L.P., Silbiger, M.L., Arrington, J.A. and Murtagh, R.F.: Validity-guided (re) clustering with applications to image segmentation. IEEE Transactions on fuzzy systems, 4(2), pp.112-123, https://doi.org/10.1109/91.493905, 1996.

Bezdek, J. C.: Pattern Recognition With Fuzzy Objective Function Algorithms, Plenum, New York, https://doi.org/10.1007/978-1-4757-0450-1_3, 1981.

Brabets, T. P., and Walvoord, M. A.: Trends in streamflow in the Yukon River Basin from 1944 to 2005 and the influence of the Pacific Decadal Oscillation. Journal of Hydrology, 371(1-4), 108-119, https://doi.org/10.1016/j.jhydrol.2009.03.018, 2009.

Brahney, J., Weber, F., Foord, V., Janmaat, J., and Curtis, P. J.: Evidence for a climate-driven hydrologic regime shift in the Canadian Columbia Basin. Canadian Water Resources Journal/Revue canadienne des ressources hydriques, 42(2), 179-192, https://doi.org/10.1080/07011784.2016.1268933, 2017.

Brimley, B., Cantin, J.F., Harvey, D., Kowalchuk, M., Marsh, P., Ouarda, T.M.B.J., Phinney, B., Pilon, P., Renouf, M., Tassone, B. and Wedel, R.: Establishment of the reference hydrometric basin network (RHBN) for Canada. Environment Canada, 41, 1999.

Brunner, M. I., Farinotti, D., Zekollari, H., Huss, M., and Zappa, M.: Future shifts in extreme flow regimes in Alpine regions, Hydrol. Earth Syst. Sci., 23, 4471–4489, https://doi.org/10.5194/hess-23-4471-2019, 2019.

Brunner, M. I., Melsen, L. A., Newman, A. J., Wood, A. W., and Clark, M. P.: Future streamflow regime changes in the United States: assessment using functional classification, Hydrol. Earth Syst. Sci., 24, 3951–3966, https://doi.org/10.5194/hess-24-3951-2020, 2020.

Brunner, M. I., Viviroli, D., Furrer, R., Seibert, J., and Favre, A. C.: Identification of flood reactivity regions via the functional clustering of hydrographs. Water Resources Research, 54(3), 1852-1867, https://doi.org/10.1002/2017WR021650, 2018.

Burn, D. H., and Whitfield, P. H.: Changes in flood events inferred from centennial length streamflow data records. Advances in Water Resources, 121, 333-349, https://doi.org/10.1016/j.advwatres.2018.08.017, 2018.

Burn, D. H.: Climatic influences on streamflow timing in the headwaters of the Mackenzie River Basin. Journal of Hydrology, 352(1-2), 225-238, https://doi.org/10.1016/j.jhydrol.2008.01.019, 2008.

Burn, D.H. and Whitfield, P.H.: Changes in cold region flood regimes inferred from long-record reference gauging stations. Water Resources Research, 53(4), pp.2643-2658, https://doi.org/10.1002/2016WR020108, 2017.

Burn, D.H. and Whitfield, P.H.: Changes in floods and flood regimes in Canada. Canadian Water Resources Journal/Revue canadienne des ressources hydriques, 41(1-2), pp.139-150, https://doi.org/10.1080/07011784.2015.1026844, 2016.

Burn, D.H., Whitfield, P.H. and Sharif, M.: Identification of changes in floods and flood regimes in Canada using a peaks over threshold approach. Hydrological Processes, 30(18), pp.3303-3314, https://doi.org/10.1002/hyp.10861, 2016.

Bush, E. and Lemmen, D.S., editors: Canada's Changing Climate Report; Government of Canada, Ottawa, ON. 444 p, 2019.

Buttle, J.M., Allen, D.M., Caissie, D., Davison, B., Hayashi, M., Peters, D.L., Pomeroy, J.W., Simonovic, S., St-Hilaire, A. and Whitfield, P.H.: Flood processes in Canada: regional and special aspects. Canadian Water Resources Journal/Revue canadienne des ressources hydriques, 41(1-2), 7-30, https://doi.org/10.1080/07011784.2015.1131629, 2016.

Champagne, O., Arain, M. A., Leduc, M., Coulibaly, P., and McKenzie, S.: Future shift in winter streamflow modulated by the internal variability of climate in southern Ontario, Hydrol. Earth Syst. Sci., 24, 3077–3096, https://doi.org/10.5194/hess-24-3077-2020, 2020.

Coops, N. C., Wulder, M. A., Duro, D. C., Han, T., and Berry, S.: The development of a Canadian dynamic habitat index using multi-temporal satellite estimates of canopy light absorbance. Ecological Indicators, 8(5), 754-766, https://doi.org/10.1016/j.ecolind.2008.01.007, 2008.

DeBeer, C. M., Wheater, H. S., Carey, S. K., and Chun, K. P..: Recent climatic, cryospheric, and hydrological changes over the interior of western Canada: a review and synthesis. Hydrology and Earth System Sciences, 20(4), 1573, https://doi.org/10.5194/hess-20-1573-2016, 2016.

Déry, S. J., and Wood, E. F.: Decreasing river discharge in northern Canada. Geophysical research letters, 32(10), https://doi.org/10.1029/2005GL022845, 2005.

Déry, S. J., Hernández-Henríquez, M. A., Owens, P. N., Parkes, M. W., and Petticrew, E. L.: A century of hydrological variability and trends in the Fraser River Basin. Environmental Research Letters, 7(2), 024019, http://dx.doi.org/10.1088/1748-9326/7/2/024019, 2012.

Déry, S. J., Mlynowski, T. J., Hernández-Henríquez, M. A., & Straneo, F.: Interannual variability and interdecadal trends in Hudson Bay streamflow. Journal of Marine Systems, 88(3), 341-351, https://doi.org/10.1016/j.jmarsys.2010.12.002, 2011.

Déry, S. J., Stadnyk, T. A., MacDonald, M. K., and Gauli-Sharma, B.: Recent trends and variability in river discharge across northern Canada, Hydrol. Earth Syst. Sci., 20, 4801–4818, https://doi.org/10.5194/hess-20-4801-2016, 2016.

Déry, S. J., Stadnyk, T. A., MacDonald, M. K., Koenig, K. A., and Guay, C.: Flow alteration impacts on Hudson Bay river discharge. Hydrological Processes, 32(24), 3576-3587, https://doi.org/10.1002/hyp.13285, 2018.

Déry, S. J., Stahl, K., Moore, R. D., Whitfield, P. H., Menounos, B., and Burford, J. E.: Detection of runoff timing changes in pluvial, nival, and glacial rivers of western Canada. Water Resources Research, 45(4), https://doi.org/10.1029/2008WR006975, 2009.

Dierauer, J. R., Allen, D. M., and Whitfield, P. H.: Climate change impacts on snow and streamflow drought regimes in four ecoregions of British Columbia, https://doi.org/10.5194/hess-2019-676, 2020.

Dierauer, J.R., Whitfield, P.H. and Allen, D.M.: Climate Controls on Runoff and Low Flows in Mountain Catchments of Western North America. Water Resources Research, https://doi.org/10.1029/2018WR023087, 2018.

Eaton, B. and Moore, R.D.: Regional hydrology. Compendium of forest hydrology and geomorphology in British Columbia, pp.85-110, 2010.

Fleming, S. W., and Clarke, G. K.: Glacial control of water resource and related environmental responses to climatic warming: empirical analysis using historical streamflow data from northwestern Canada. Canadian Water Resources Journal, 28(1), 69-86, https://doi.org/10.4296/cwrj2801069, 2003.

Fleming, S. W., and Weber, F. A.: Detection of long-term change in hydroelectric reservoir inflows: Bridging theory and practise. Journal of Hydrology, 470, 36-54, https://doi.org/10.1016/j.jhydrol.2012.08.008, 2012.

Forbes, W. L., Mao, J., Ricciuto, D. M., Kao, S. C., Shi, X., Tavakoly, A. A., Jin, M., Guo, W., Zhao, T., Wang, Y., Thornton, P. E. and Hoffman, F., M.: Streamflow in the Columbia River Basin: Quantifying changes over the period 1951-2008 and determining the drivers of those changes. Water Resources Research, 55(8), 6640-6652, https://doi.org/10.1029/2018WR024256, 2019.

Fukuyama, Y., Sugeno, M.: A new method of choosing the number of clusters for the fuzzy c-mean method. In: Proc. 5th Fuzzy Syst. Symp., pp. 247–250, 1989, (in Japanese).

Genest, C., and Favre, A. C.: Everything you always wanted to know about copula modeling but were afraid to ask. Journal of hydrologic engineering, 12(4), 347-368, https://doi.org/10.1061/(ASCE)1084-0699(2007)12:4(347), 2007.

Guetter, A. K., and Georgakakos, K. P.: River outflow of the conterminous United States, 1939–1988. Bulletin of the American Meteorological Society, 74(10), 1873-1892, https://doi.org/10.1175/1520-0477(1993)074%3C1873:ROOTCU%3E2.0.CO;2, 1993.

Hall, J., Arheimer, B., Borga, M., Brázdil, R., Claps, P., Kiss, A., Kjeldsen, T. R., Kriaučiūnienė, J., Kundzewicz, Z. W., Lang, M., Llasat, M. C., Macdonald, N., McIntyre, N., Mediero, L., Merz, B., Merz, R., Molnar, P., Montanari, A., Neuhold, C., Parajka, J., Perdigão, R. A. P., Plavcová, L., Rogger, M., Salinas, J. L., Sauquet, E., Schär, C., Szolgay, J., Viglione, A., and

Blöschl, G.: Understanding flood regime changes in Europe: a state-of-the-art assessment, Hydrol. Earth Syst. Sci., 18, 2735-2772, https://doi.org/10.5194/hess-18-2735-2014, 2014.

Hamududu, B., and Killingtveit, A.: Assessing climate change impacts on global hydropower. Energies, 5(2), 305-322, https://dx.doi.org/10.3390/en5020305, 2012.

Hannachi, A., Unkel, S., Trendafilov, N. T., and Jolliffe, I. T.: Independent component analysis of climate data: a new look at EOF rotation. Journal of Climate, 22(11), 2797-2812, https://doi.org/10.1175/2008JCLI2571.1, 2009.

Harvey, K.D., Pilon, P.J. and Yuzyk, T.R.: Canada's reference hydrometric basin network (RHBN). In Proceedings of the CWRA 51st Annual Conference, Nova Scotia, 1999.

Hassanzadeh, E., Elshorbagy, A., Nazemi, A., Jardine, T. D., Wheater, H., and Lindenschmidt, K. E.: The ecohydrological vulnerability of a large inland delta to changing regional streamflows and upstream irrigation expansion. Ecohydrology, 10(4), e1824, https://doi.org/10.1002/eco.1824, 2017.

Hatami, S., Zandmoghaddam, S. and Nazemi, A.: Statistical Modeling of Monthly Snow Depth Loss in Southern Canada, J. Hydrol. Eng., https://doi.org/10.1061/(ASCE)HE.1943-5584.0001763, 2018.

Hock, R., Jansson, P., and Braun, L. N.: Modelling the response of mountain glacier discharge to climate warming. In Global Change and Mountain Regions (pp. 243-252). Springer, Dordrecht, https://doi.org/10.1007/1-4020-3508-X_25, 2005.

Hodgkins, G.A., Whitfield, P.H., Burn, D.H., Hannaford, J., Renard, B., Stahl, K., Fleig, A.K., Madsen, H., Mediero, L., Korhonen, J. and Murphy, C.: Climate-driven variability in the occurrence of major floods across North America and Europe. Journal of Hydrology, 552, pp.704-717, https://doi.org/10.1016/j.jhydrol.2017.07.027, 2017.

Ireson, A.M., Barr, A.G., Johnstone, J.F., Mamet, S.D., Van der Kamp, G., Whitfield, C.J., Michel, N.L., North, R.L., Westbrook, C.J., DeBeer, C. and Chun, K.P.: The changing water cycle: the Boreal Plains ecozone of Western Canada. Wiley Interdisciplinary Reviews: Water, 2(5), pp.505-521, https://doi.org/10.1002/wat2.1098, 2015.

Islam, S. U., Curry, C. L., Déry, S. J., and Zwiers, F. W.: Quantifying projected changes in runoff variability and flow regimes of the Fraser River Basin, British Columbia, Hydrol. Earth Syst. Sci., 23, 811–828, https://doi.org/10.5194/hess-23-811-2019, 2019.

Janowicz, J.R.: Apparent recent trends in hydrologic response in permafrost regions of northwest Canada. Hydrology Research, 39(4), pp.267-275, https://doi.org/10.2166/nh.2008.103, 2008.

Janowicz, J.R.: Streamflow responses and trends between permafrost and glacierized regimes in northwestern Canada. IAHS Publ, 346, pp.9-14, 2011.

Jaramillo, P. and Nazemi, A.: Assessing urban water security under changing climate: Challenges and ways forward. Sustainable cities and society, 41, pp.907-918, https://doi.org/10.1016/j.scs.2017.04.005, 2018.

Jehn, F. U., Bestian, K., Breuer, L., Kraft, P., and Houska, T.: Using hydrological and climatic catchment clusters to explore drivers of catchment behavior, Hydrol. Earth Syst. Sci., 24, 1081–1100, https://doi.org/10.5194/hess-24-1081-2020, 2020.

Johnston, C. A., and Shmagin, B. A.: Regionalization, seasonality, and trends of streamflow in the US Great Lakes Basin. Journal of Hydrology, 362(1-2), 69-88, https://doi.org/10.1016/j.jhydrol.2008.08.010, 2008.

Kang, D. H., Gao, H., Shi, X., ul Islam, S., and Déry, S. J.: Impacts of a rapidly declining mountain snowpack on streamflow timing in Canada's Fraser River basin. Scientific reports, 6, 19299, https://doi.org/10.1038/srep19299, 2016.

Kendall, M. G.: Rank Correlation Methods. Griffin & Co, London. ISBN 0-85264-199-0, 1975.

Kingston, D. G., Hannah, D. M., Lawler, D. M., and McGregor, G. R.: Regional classification, variability, and trends of northern North Atlantic river flow. Hydrological Processes, 25(7), 1021-1033. https://doi.org/10.1002/hyp.7655, 2011.

Knoben, W.J., Woods, R.A. and Freer, J.E.: A Quantitative Hydrological Climate Classification Evaluated With Independent Streamflow Data. Water Resources Research, 54(7), pp.5088-5109, https://doi.org/10.1029/2018WR022913, 2018.

Knouft, J. H., and Ficklin, D. L.: The potential impacts of climate change on biodiversity in flowing freshwater systems. Annual Review of Ecology, Evolution, and Systematics, 48, 111-133, https://doi.org/10.1146/annurev-ecolsys-110316-022803, 2017.

Kuentz, A., Arheimer, B., Hundecha, Y., and Wagener, T.: Understanding hydrologic variability across Europe through catchment classification, Hydrol. Earth Syst. Sci., 21, 2863–2879, https://doi.org/10.5194/hess-21-2863-2017, 2017.

Legates, D. R., and McCabe Jr, G. J.: Evaluating the use of "goodness-of-fit" measures in hydrologic and hydroclimatic model validation. Water resources research, 35(1), 233-241, https://doi.org/10.1029/1998WR900018, 1999.

MacDonald, M.K., Stadnyk, T.A., Déry, S.J., Braun, M., Gustafsson, D., Isberg, K. and Arheimer, B.: Impacts of 1.5 and 2.0° C Warming on Pan-Arctic River Discharge Into the Hudson Bay Complex Through 2070. Geophysical Research Letters, 45(15), pp.7561-7570, https://doi.org/10.1029/2018GL079147, 2018.

Mann, H. B.: Nonparametric Tests Against Trend. Econometrica, 13(3), 245. https://doi.org/10.2307/1907187, 1945.

Matalas, N. C., and Reiher, B. J.: Some comments on the use of factor analyses. Water resources research, 3(1), 213-223, https://doi.org/10.1029/WR003i001p00213, 1967.

Marshall, I.B., Schut, P.H., and Ballard, M.: A National Ecological Framework for Canada: Attribute Data. Agriculture and Agri-Food Canada, Research Branch, Centre for Land and Biological Resources Research and Environment Canada, State of the Environment Directorate, Ecozone Analysis Branch. Ottawa/Hull, 1999.

Maurer, E. P., Lettenmaier, D. P., and Mantua, N. J.: Variability and potential sources of predictability of North American runoff. Water Resources Research, 40(9), https://doi.org/10.1029/2003WR002789, 2004.

Milly, P. C., Betancourt, J., Falkenmark, M., Hirsch, R. M., Kundzewicz, Z. W., Lettenmaier, D. P., and Stouffer, R. J.: Stationarity is dead: Whither water management?. Science, 319(5863), 573-574, https://doi.org/10.1126/science.1151915, 2008.

Moore, R. D., Trubilowicz, J. W., and Buttle, J. M.: Prediction of Streamflow Regime and Annual Runoff for Ungauged Basins Using a Distributed Monthly Water Balance Model 1. JAWRA Journal of the American Water Resources Association, 48(1), 32-42, https://doi.org/10.1111/j.1752-1688.2011.00595.x, 2012.

Natural Resources Canada.: The Atlas of Canada: Lakes, Rivers and Names of Canada, online at https://open.canada.ca/data/en/dataset/e625c0b0-2d5f-50d8-9e0c-a6e0fd5876ee, 2007.

Nazemi, A. R., Akbarzadeh, M. R., and Hosseini, S. M.: Fuzzy-stochastic linear programming in water resources engineering. 2002 Annual Meeting of the North American Fuzzy Information Processing Society Proceedings. NAFIPS-FLINT 2002 (Cat. No. 02TH8622) (pp. 227-232). IEEE, https://doi.org/10.1109/NAFIPS.2002.1018060, 2002.

Nazemi, A. A., and Wheater, H. S.: Assessing the vulnerability of water supply to changing streamflow conditions. Eos, Transactions American Geophysical Union, 95(32), 288-288, https://doi.org/10.1002/2014EO320007, 2014.

Nazemi, A., and Elshorbagy, A.: Application of copula modelling to the performance assessment of reconstructed watersheds. Stochastic environmental research and risk assessment, 26(2), 189-205, https://doi.org/10.1007/s00477-011-0467-7, 2012.

Nazemi, A., and Wheater, H. S.: On inclusion of water resource management in Earth system models—Part 1: Problem definition and representation of water demand. Hydrology and Earth System Sciences, 19, 33–61. https//doi.org/105194/hess-19-33-2015, 2015a.

Nazemi, A., and Wheater, H. S.: On inclusion of water resource management in Earth system models—Part 2: Representation of water supply and allocation and opportunities for improved modeling. Hydrology and Earth System Sciences, 19, 63–90. https://doi.org/10.5194/hess-19-63-2015, 2015b.

Nazemi, A., Wheater, H. S., Chun, K. P., Bonsal, B., and Mekonnen, M.: Forms and drivers of annual streamflow variability in the headwaters of Canadian Prairies during the 20th century. Hydrological processes, 31(1), 221-239, https://doi.org/10.1002/hyp.11036, 2017.

Nazemi, A., Zaerpour, M., and Hassanzadeh, E.: Uncertainty in Bottom-Up Vulnerability Assessments of Water Supply Systems due to Regional Streamflow Generation under Changing Conditions. Journal of Water Resources Planning and Management, 146(2), 04019071, https://doi.org/10.1061/(ASCE)WR.1943-5452.0001149 ,2020.

Olden, J.D. and Poff, N.L.: Redundancy and the choice of hydrologic indices for characterizing streamflow regimes. River Research and Applications, 19(2), pp.101-121, https://doi.org/10.1002/rra.700, 2003.

Olden, J.D., Kennard, M.J. and Pusey, B.J.: A framework for hydrologic classification with a review of methodologies and applications in ecohydrology. Ecohydrology, 5(4), pp.503-518, https://doi.org/10.1002/eco.251, 2012.

O'Neil, H. C. L., Prowse, T. D., Bonsal, B. R., and Dibike, Y. B.: Spatial and temporal characteristics in streamflow-related hydroclimatic variables over western Canada. Part 1: 1950–2010. Hydrology Research, 48(4), 915-931, https://doi.org/10.2166/nh.2016.057, 2017.

Overland, J. E., and Preisendorfer, R. W.: A significance test for principal components applied to a cyclone climatology. Monthly Weather Review, 110(1), 1-4, https://doi.org/10.1175/1520-0493(1982)110%3C0001:ASTFPC%3E2.0.CO;2, 1982.

Pearse, P.H., F. Bertrand and J.W. MacLaren.: Currents of Change: Final Report of the Inquiry on Federal Water Policy, Environment Canada, Ottawa, 1985.

Pike, R.G., T.E. Redding, R.D. Moore, R.D. Winker and K.D. Bladon editors.: Compendium of forest hydrology and geomorphology in British Columbia. B.C. Min. For. Range, For. Sci. Prog., Victoria, B.C. and FORREX Forum for Research and Extension in Natural Resources, Kamloops, B.C. Land Manag. Handb. 66. www.for.gov.bc.ca/hfd/pubs/Docs/Lmh/Lmh66.htm, 2010.

Poff, N.L., Allan, J.D., Bain, M.B., Karr, J.R., Prestegaard, K.L., Richter, B.D., Sparks, R.E. and Stromberg, J.C.: The natural flow regime. BioScience, 47(11), pp.769-784, https://doi.org/10.2307/1313099, 1997.

Poff, N.L., Richter, B.D., Arthington, A.H., Bunn, S.E., Naiman, R.J., Kendy, E., Acreman, M., Apse, C., Bledsoe, B.P., Freeman, M.C. and Henriksen, J.: The ecological limits of hydrologic alteration (ELOHA): a new framework for developing regional environmental flow standards. Freshwater Biology, 55(1), 147-170, https://doi.org/10.1111/j.1365-2427.2009.02204.x, 2010.

Power, K., and Gillis, M. D.: Canada's forest inventory 2001 (Vol. 408). Pacific Forestry Centre, 2006.

Richter, B.D., Baumgartner, J.V., Powell, J. and Braun, D.P.: A method for assessing hydrologic alteration within ecosystems. Conservation biology, 10(4), pp.1163-1174, https://doi.org/10.1046/j.1523-1739.1996.10041163.x, 1996.

Rood, S. B., Foster, S. G., Hillman, E. J., Luek, A., and Zanewich, K. P.: Flood moderation: Declining peak flows along some Rocky Mountain rivers and the underlying mechanism. Journal of Hydrology, 536, 174-182, https://doi.org/10.1016/j.jhydrol.2016.02.043, 2016.

Rood, S. B., Pan, J., Gill, K. M., Franks, C. G., Samuelson, G. M., & Shepherd, A.: Declining summer flows of Rocky Mountain rivers: Changing seasonal hydrology and probable impacts on floodplain forests. Journal of Hydrology, 349(3-4), 397-410, https://doi.org/10.1016/j.jhydrol.2007.11.012, 2008.

Rottler, E., Francke, T., Bürger, G., and Bronstert, A.: Long-term changes in central European river discharge for 1869–2016: impact of changing snow covers, reservoir constructions and an intensified hydrological cycle, Hydrol. Earth Syst. Sci., 24, 1721–1740, https://doi.org/10.5194/hess-24-1721-2020, 2020.

Rowe, J. S., and Sheard, J. W.: Ecological land classification: a survey approach. Environmental management, 5(5), 451-464, https://doi.org/10.1007/BF01866822, 1981.

Satopaa, V., Albrecht, J., Irwin, D., & Raghavan, B.: Finding a" kneedle" in a haystack: Detecting knee points in system behavior. In 2011 31st international conference on distributed computing systems workshops (pp. 166-171). IEEE, https://10.1109/ICDCSW.2011.20, 2011.

Schnorbus, M., Werner, A. and Bennett, K.: Impacts of climate change in three hydrologic regimes in British Columbia, Canada. Hydrological Processes, 28(3), pp.1170-1189, https://doi.org/10.1002/hyp.9661, 2014.

Sen, P. K.: Estimates of the regression coefficient based on Kendall's tau. Journal of the American statistical association, 63(324), 1379-1389, http://dx.doi.org/10.1080/01621459.1968.10480934, 1968.

Sikorska, A. E., Viviroli, D., and Seibert, J.: Flood-type classification in mountainous catchments using crisp and fuzzy decision trees. Water Resources Research, 51(10), 7959-7976, https://doi.org/10.1002/2015WR017326, 2015.

Smith, L. C., Pavelsky, T. M., MacDonald, G. M., Shiklomanov, A. I., and Lammers, R. B.: Rising minimum daily flows in northern Eurasian rivers: A growing influence of groundwater in the high-latitude hydrologic cycle. Journal of Geophysical Research: Biogeosciences, 112(G4), https://doi.org/10.1029/2006JG000327, 2007.

Spence, C., and Phillips, R. W.: Refining understanding of hydrological connectivity in a boreal catchment. Hydrological Processes, 29(16), 3491-3503, https://doi.org/10.1002/hyp.10270, 2015.

Srinivas, V. V., Tripathi, S., Rao, A. R., and Govindaraju, R. S.: Regional flood frequency analysis by combining self-organizing feature map and fuzzy clustering. Journal of Hydrology, 348(1-2), 148-166. https://doi.org/10.1016/j.jhydrol.2007.09.046, 2008.

St. Jacques, J. M., and Sauchyn, D. J.: Increasing winter baseflow and mean annual streamflow from possible permafrost thawing in the Northwest Territories, Canada. Geophysical Research Letters, 36(1), https://doi.org/10.1029/2008GL035822, 2009.

Stahl, K. and Moore, R.D.: Influence of watershed glacier coverage on summer streamflow in British Columbia, Canada. Water Resources Research, 42(6), https://doi.org/10.1029/2006WR005022, 2006.

Stahl, K., Hisdal, H., Hannaford, J., Tallaksen, L. M., van Lanen, H. A. J., Sauquet, E., Demuth, S., Fendekova, M., and Jódar, J.: Streamflow trends in Europe: evidence from a dataset of near-natural catchments, Hydrol. Earth Syst. Sci., 14, 2367-2382, https://doi.org/10.5194/hess-14-2367-2010, 2010.

Tarasova, L., Merz, R., Kiss, A., Basso, S., Blöschl, G., Merz, B., Viglione, A., Plötner, S., Guse, B., Schumann, A. and Fischer, S.: Causative classification of river flood events. Wiley Interdisciplinary Reviews: Water, 6(4), p.e1353, https://doi.org/10.1002/wat2.1353, 2019.

Ternynck, C., Ben Alaya, M. A., Chebana, F., Dabo-Niang, S., and Ouarda, T. B.: Streamflow hydrograph classification using functional data analysis. Journal of hydrometeorology, 17(1), 327-344, https://doi.org/10.1175/JHM-D-14-0200.1, 2016.

Thistle M.E. and Caissie, D.: Trends in air temperature, total precipitation, and streamflow characteristics in eastern Canada. Can. Tech. Rep. Fish. Aquat. Sci. 3018: xi + 97p., 2013.

Thorne, R., and Woo, M. K.: Streamflow response to climatic variability in a complex mountainous environment: Fraser River Basin, British Columbia, Canada. Hydrological Processes, 25(19), 3076-3085, https://doi.org/10.1002/hyp.8225, 2011.

Trunk, G. V.: A problem of dimensionality: A simple example. IEEE Transactions on pattern analysis and machine intelligence, (3), 306-307, https://doi.org/10.1109/TPAMI.1979.4766926, 1979.

Vormoor, K., Lawrence, D., Heistermann, M. and Bronstert, A.: Climate change impacts on the seasonality and generation processes of floods–projections and uncertainties for catchments with mixed snowmelt/rainfall regimes. Hydrology and Earth System Sciences, 19(2), pp.913-931, https://doi.org/10.5194/hess-19-913-2015, 2015.

Wade, N.L., Martin, J. and Whitfield, P.H.: Hydrologic and climatic zonation of Georgia basin, British Columbia. Canadian Water Resources Journal, 26(1), pp.43-70, https://doi.org/10.4296/cwrj2601043, 2001.

Walvoord, M. A., and Striegl, R. G.: Increased groundwater to stream discharge from permafrost thawing in the Yukon River basin: Potential impacts on lateral export of carbon and nitrogen. Geophysical Research Letters, 34(12), https://doi.org/10.1029/2007GL030216, 2007.

Wang, X., Yang, T., Yong, B., Krysanova, V., Shi, P., Li, Z., and Zhou, X.: Impacts of climate change on flow regime and sequential threats to riverine ecosystem in the source region of the Yellow River. Environmental Earth Sciences, 77(12), 465, https://doi.org/10.1007/s12665-018-7628-7, 2018.

Whitfield, P. H., and Cannon, A. J.: Recent variations in climate and hydrology in Canada. Canadian Water Resources Journal, 25(1), 19-65, https://doi.org/10.4296/cwrj2501019, 2000.

Whitfield, P. H., and Pomeroy, J. W.: Changes to flood peaks of a mountain river: implications for analysis of the 2013 flood in the Upper Bow River, Canada. Hydrological Processes, 30(25), 4657-4673, https://doi.org/10.1002/hyp.10957, 2016.

Whitfield, P. H., Shook, K. R., and Pomeroy, J. W.: Spatial patterns of temporal changes in Canadian Prairie streamflow using an alternative trend assessment approach. Journal of Hydrology, 582, 124541, https://doi.org/10.1016/j.jhydrol.2020.124541, 2020.

Whitfield, P.H.: Linked hydrologic and climate variations in British Columbia and Yukon. Environmental Monitoring and Assessment. 67, 217-238, https://doi.org/10.1023/A:1006438723879, 2001.

Wiken, E. B.: Terrestrial ecozones of Canada. Environment Canada, Lands Directorate, 1986.

Wolfe, J. D., Shook, K. R., Spence, C., and Whitfield, C. J.: A watershed classification approach that looks beyond hydrology: application to a semi-arid, agricultural region in Canada, Hydrol. Earth Syst. Sci., 23, 3945–3967, https://doi.org/10.5194/hess-23-3945-2019, 2019.

Wong, J. S., Razavi, S., Bonsal, B. R., Wheater, H. S., and Asong, Z. E.: Inter-comparison of daily precipitation products for large-scale hydro-climatic applications over Canada, Hydrol. Earth Syst. Sci., 21, 2163–2185, https://doi.org/10.5194/hess-21-2163-2017, 2017.

Woo, M. K., Thorne, R., Szeto, K., and Yang, D.: Streamflow hydrology in the boreal region under the influences of climate and human interference. Philosophical Transactions of the Royal Society B: Biological Sciences, 363(1501), 2249-2258, https://doi.org/10.1098/rstb.2007.2197, 2008.

Xie, X.L., Beni, G.A.: Validity measure for fuzzy clustering. IEEE Trans. PAMI 3(8), 841–846, https://doi.ieeecomputersociety.org/10.1109/34.85677, 1991.

Yang, D., Shi, X., and Marsh, P.: Variability and extreme of Mackenzie River daily discharge during 1973–2011. Quaternary International, 380, 159-168, https://doi.org/10.1016/j.quaint.2014.09.023, 2015.

Yue, S., Pilon, P., and Phinney, B. O. B.: Canadian streamflow trend detection: impacts of serial and cross-correlation. Hydrological Sciences Journal, 48(1), 51-63, https://doi.org/10.1623/hysj.48.1.51.43478, 2003.

Zadeh, L. A.: Fuzzy sets. Information and control, 8(3), 338-353, https://doi.org/10.1016/S0019-9958(65)90241-X, 1965.

Zandmoghaddam, S., Nazemi, A., Hassanzadeh, E., and Hatami, S.: Representing local dynamics of water resource systems through a data-driven emulation approach. Water Resources Management, 33(10), 3579-3594, https://doi.org/10.1007/s11269-019-02319-3, 2019.